Supplemental Data

Tracer Synthesis

To incorporate a small fluorine containing substituent in the R^4 position, the synthetic route depicted in Figure 2 was used. Based on the idea from rational design, we decided to incorporate fluoroethoxy group on phenyl group at the western part of the quinazolinone core, as fluoroethoxy group is not too bulky while it is readily to be radiolabelled. Compounds **4-7a** and **4-7b** were synthesized according to Figure 2. 2-Amino-5-bromobenzoic acid was treated with 2,4-Difluorobenzoyl chloride to form benzoxazinone **1**. The addition of BOC-protected aminomethylpiperidine provided uncyclized product **2**, which was cyclized under ethylene glycol via microwave irradiation to give compound **3**. An hydroxyethoxy group was introduced during this step via nucleophilic aromatic substitution of the para-fluorine due to the electron withdrawing effect of the other fluorine at ortho position. It was followed by Ullmann coupling reactions and Boc-deprotecion to furnish compound **4a** and **4b**. Alkylation with 2-bromopropane were then performed to furnish compound **5a** and **5b**. Ytterbium(III) catalyzed tosylation on the hydroxyl group led to compound **6a** and **6b**, which was followed by fluorination to furnish compound **7a** and **7b**.

^{18}F Radiochemistry

Compound **7b** showed excellent binding affinity (IC_{50}: 0.33nM) and cLogD (cLog D: 2.53). Using compound **6b** as precursor (Scheme 6), it was successfully ^{18}F-radiolabeled in one step with a decay corrected radiochemical yield of 8 ± 4%, molar activity of 87 ± 64 GBq/μmol and a radio-purity of > 99% (n = 11).

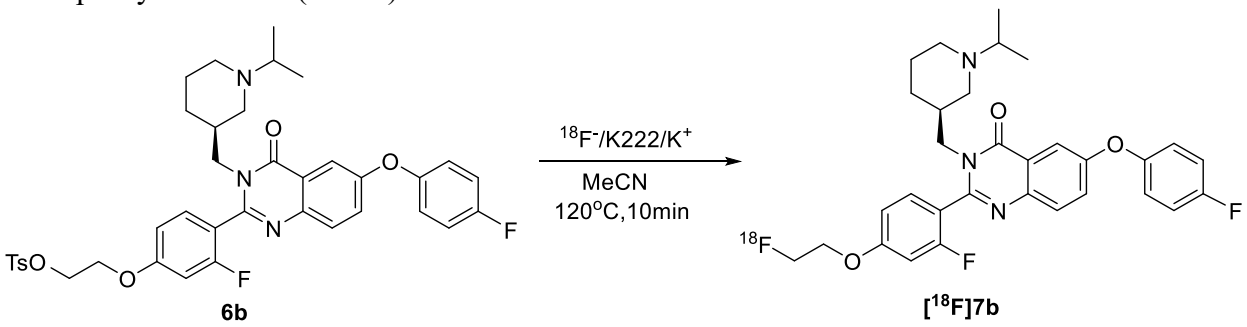

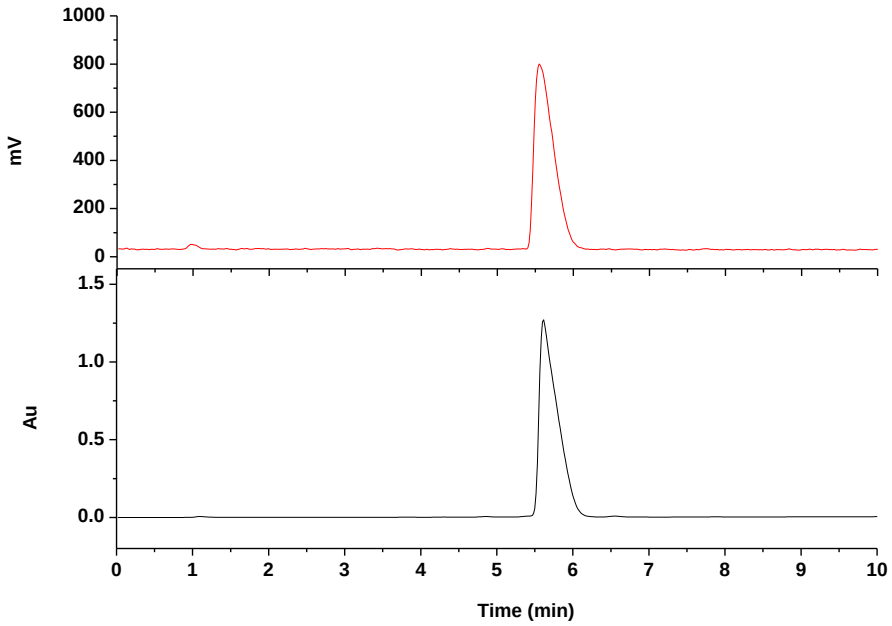

Supplemental Figure 1. Radio-synthesis of **[^{18}F]7b** (top panel). Stacked HPLC chromatograms (λ = 254 nm) (bottom line) and radio chromatograms (top line) for **7b** and **[^{18}F]7b** (bottom panel).

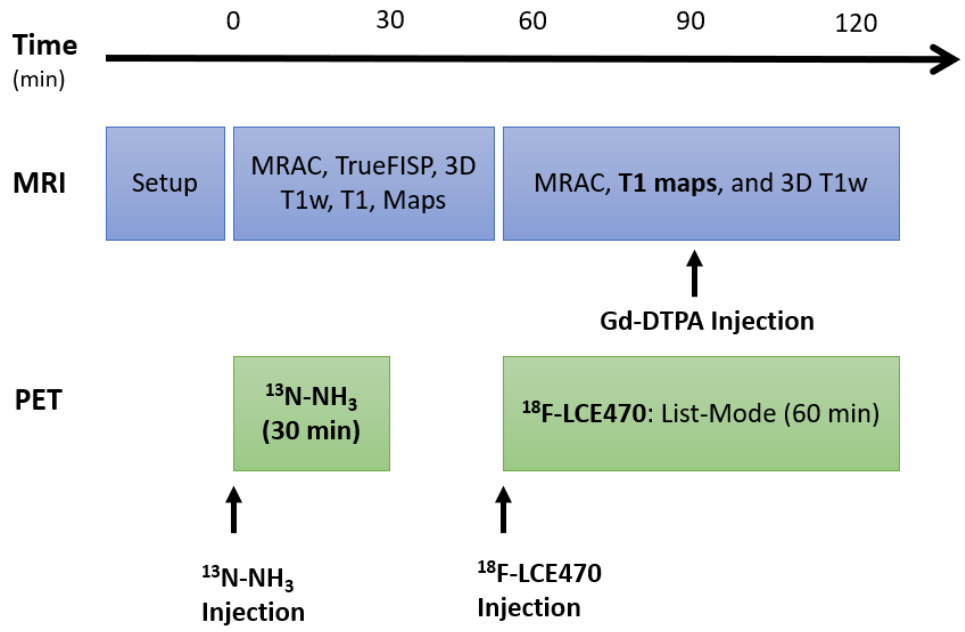

Supplemental Figure 2. PET/MR Imaging Schematic.

Briefly, anesthesia was induced with propofol and maintained with 1.5 – 2.0% isoflurane. The heart was exposed through a left thoracotomy. The mid portion of the left anterior descending coronary artery (LAD) was isolated just distal to the first diagonal branch and occluded by a thread ligature for 3 h, followed by reperfusion by release of the ligature. After 1 h of reperfusion, the chest wall was closed. All hounds were allowed to recover for 24 h before the first post-surgery imaging session. All hounds were part of a cohort of another study and were administered an oral iron chelator twice daily for 30 days after MI starting on the day of surgery [22].

Positron Emission Tomography/ Magnetic Resonance Imaging

Simultaneous PET/MR imaging was performed one week prior to surgery, and at multiple time points post-surgery over a period of 1.5 years as illustrated in Supplemental Figure 1. On the day of the imaging session, hounds were anesthetized as described above and placed onto the bed of

a 3T Biograph mMR (Siemens Medical Solutions, Erlangen, Germany). A hind leg catheter was inserted for injection of PET tracers and Gd-DTPA. Technical issues such as data corruption of either the PET or cMRI sequences, tracer production failure and early sacrifice for one hound prevented both [^{18}F]LCE470 and [^{13}N]NH_3 PET imaging of all hounds at all time points.

^{13}N-NH_3 Data Acquisition

Hounds were imaged at the following time points post-surgery: Day 21 (n=3), Week 16 (n=4), Month 11 (n=3). A 30-minute dynamic list-mode PET acquisition was initiated simultaneously with a bolus injection of 6.5 – 7 MBq/kg of ^{13}N-NH_3 (produced in-house at the Lawson Cyclotron Facility). PET data were reconstructed using a 3D Ordered Subset Expectation Maximization reconstruction (3 iterations, 21 subsets, 172 x 172 x 127 matrix size, zoom of 2, and 4 mm Gaussian filter) in the following segments: 12 frames x 10 seconds, 2 frames x 30 seconds, 1 frame x 60 seconds, 1 frame x 360 seconds. An MR-based attenuation correction was used from a two-point Dixon MRI sequence that was segmented into water, fat, lung, and air with constant attenuation coefficients for each tissue listed. PET voxel size was 2.09 x 2.09 x 2.03mm.

[^{18}F]LCE470 Data Acquisition

Fifty minutes following ^{13}N-NH_3 imaging, hounds were imaged with [^{18}F]LCE470 at the following time points: baseline (n=3), day 3 (n=4), Day 21 (n=3), Week 16 (n=4), Month 11 (n=3) (Supplemental Figure 1). A 60-minute dynamic list mode PET acquisition was started simultaneously with a bolus injection of 6.5 – 7 MBq/kg of [^{18}F]LCE470 in the hind leg catheter. Data were decay-corrected to the time of injection, and images were corrected for dead time, and random and scatter coincidences. PET data was reconstructed using OSEM as above in the

following segments for a dynamic scan: 12 frames x 10 seconds, 6 frames x 30 seconds, 5 frames x 60 seconds, 10 frames x 300 seconds. PET data was also reconstructed from the last 15 minutes of the scan to generate a static image for determination of standardized uptake values (SUVs). An MR-based attenuation correction was used as above. PET voxel size was 2.09 x 2.09 x 2.03mm. On days when ^{13}N-NH_3 was not injected, [^{18}F]LCE470 was injected at time 0 and PET/MR imaging was conducted for 60 min.

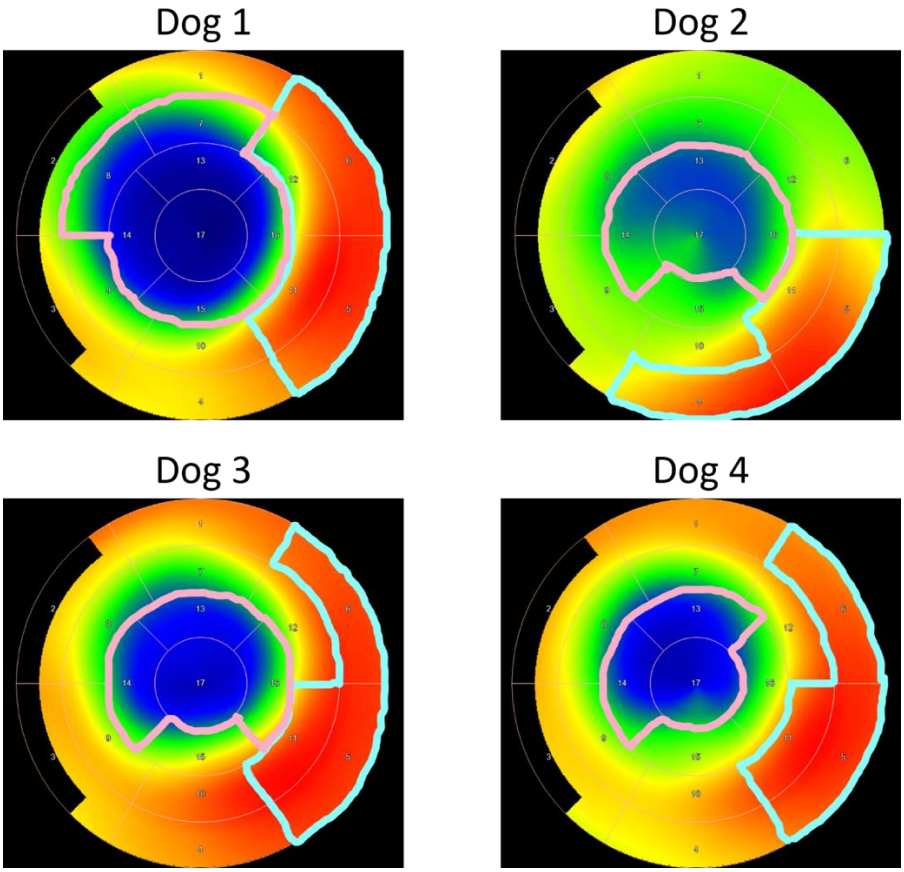

Supplemental Figure 3. Segmentation of the left ventricular region and definition of regions of interest (ROIs). The reconstructed dynamic data from the left ventricle was used to segment the area of the LV automatically. Manual corrections were made based on tissue localization in each axis (coronal short axis, vertical long axis, horizontal long axis) and slice. Regions of

interest (ROIs) were determined using images from day 3 post-surgery, and these same ROIs were used throughout all scans. The ROIs representing the area of infarct, left circumflex region, remote myocardium and the blood pool were manually delineated using Matlab R2020a software with custom scripts. The left circumflex region is outlined in light blue and the area of infarct outlined in pink. The remote tissue consisted of all other segments not outlined. ROIs were determined for all dogs at day 3 post-surgery and were precisely the same ROIs used throughout all scans. To generate time-activity curves for each region and at each time point, dynamically-acquired list mode data were uploaded to the online software package Carimas 2.10.0.0 (Turku Pet Center, Hospital District of Southwest Finland, https://turkupetcentre.fi/carimas/). Standardized uptake values (SUVs) for [^{18}F]LCE470 and ^{13}N-NH_3 were used to calculate tissue to blood ratios (TBR) using the online software 3D Slicer 4.8.1 (https://www.slicer.org/). PET and gadolinium-enhanced T1 MR images were uploaded and regions of interest (ROIs) as described above were manually drawn onto the MR images. The 2D ROIs were then transferred to the corresponding PET slices. The SUVs for each ROI were determined as follows: tissue activity (MBq/ml)/ injected dose (MBq) X body weight (g). TBR was automatically calculated for each hound at each time point using the following formula:

(1):

$$TBR: \frac{SUV_{tissue\ ROI}\left(\frac{g}{ml}\right)}{SUV_{blood\ pool}\left(\frac{g}{ml}\right)}$$

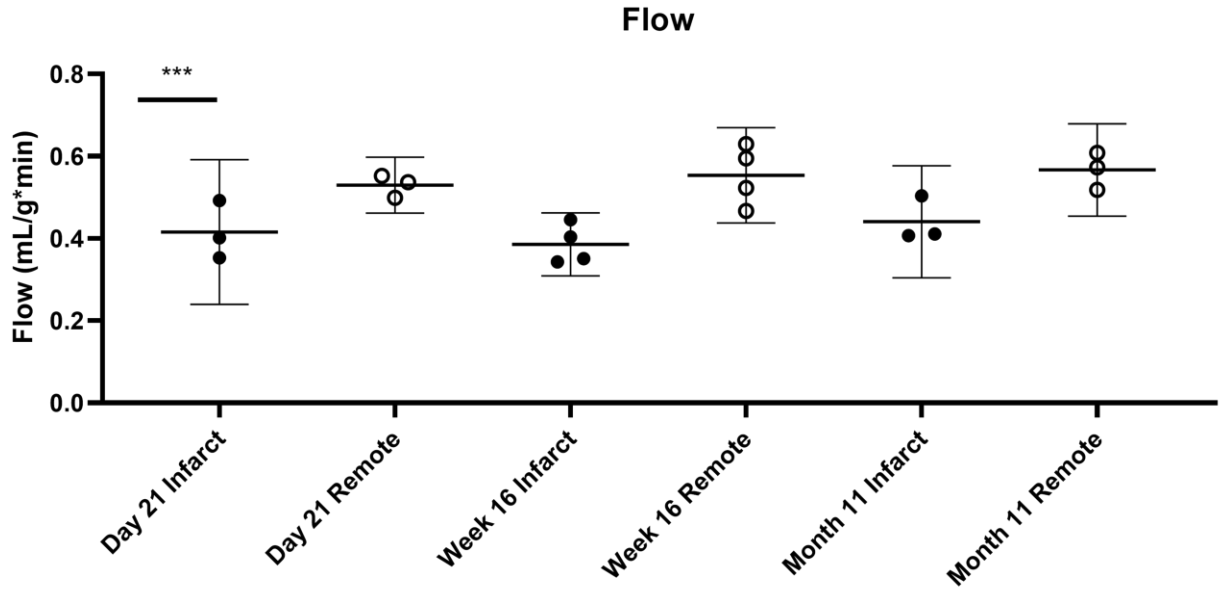

Supplemental Figure 4. Changes in absolute myocardial blood flow in remote myocardium and area of infarct.

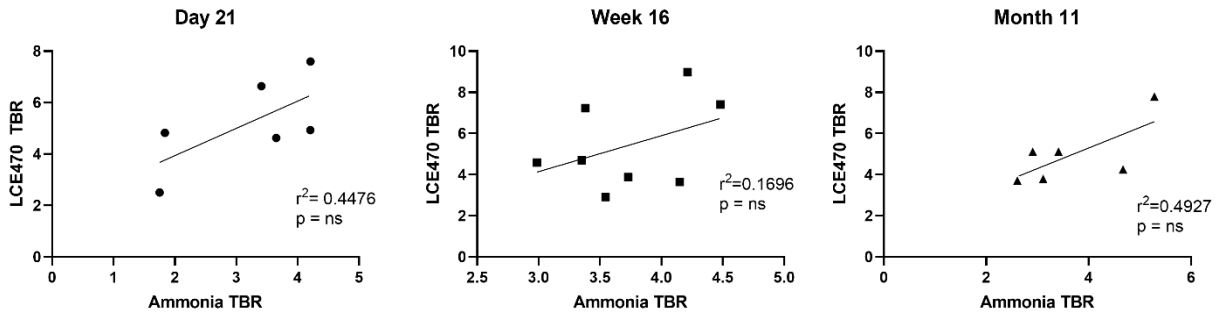

Supplemental Figure 5. Correlation of [^{18}F]LCE470 and ^{13}N-NH$_3$. In order to determine the relationship between [^{18}F]LCE470 uptake and myocardial perfusion, linear regressions were performed between TBRs of [^{18}F]LCE470 and ^{13}N-NH$_3$. Values from remote and left circumflex areas were selected for analysis; values from the infarct region were not used as tracer uptake in this area was significantly decreased and would therefore skew the regression analysis. Data from day 21, week 16 and month 11 were selected, as these were the time points at which both tracers were injected. Data derived from the remote and left circumflex tissues from all dogs were pooled. A) Linear regression analysis of TBR values showed no correlation at any given time point. B) Linear regression analysis showed no significant correlation between tracer patterns in the remote and circumflex areas at any time point.

	EF	ESV	EDV	SV	ESM	EDM
Baseline	41.3 ± 9.6	23.7 ± 3.0	40.7 ± 3.7	17.0 ± 5.4	63.9 ± 9.5	62.1 ± 8.7
Day 1	26.8 ± 6.2	29.3 ± 8.2	39.5 ± 8.1	10.1 ± 0.9	66.1 ± 12.2	63.3 ± 12.0
Day 3	27.7 ± 7.1	29.0 ± 3.8	40.4 ± 7.8	11.5 ± 4.5	71.6 ± 13.3	69.1 ± 10.6
Day 7	35.3 ± 0.4	24.9 ± 1.5	38.5 ± 2.4	13.6 ± 0.9	68.0 ± 7.6	68.4 ± 8.6
Day 21	37.9 ± 1.9	20.9 ± 4.8	33.7 ± 8.1	12.8 ± 3.4	60.6 ± 8.2	60.5 ± 8.5
Day 28	36.5 ± 2.8	22.8 ± 2.4	36.0 ± 4.5	13.2 ± 2.4	59.3 ± 8.8	58.5 ± 7.8
Week 8	34.9 ± 2.6	26.6 ± 5.2	40.9 ± 8.1	14.3 ± 3.3	58.5 ± 8.6	58.3 ± 8.3
Week 16	34.5 ± 3.0	25.7 ± 4.4	39.4 ± 8.5	13.7 ± 4.2	56.9 ± 15.2	56.3 ± 15.3
Mo 6	32.2 ± 1.4	27.7 ± 4.0	40.9 ± 6.4	13.2 ± 2.5	54.6 ± 2.2	53.9 ± 2.1
Mo 11	36.9 ± 10.3	38.1 ± 2.2	61.3 ± 9.3	23.2 ± 10.1	53.2 ± 10.1	53.5 ± 4.2
Mo12	31.5 ± 4.5	41.0 ± 2.4	60.0 ± 4.4	19.0 ± 3.7	53.0 ± 3.7	52.0 ± 5.5

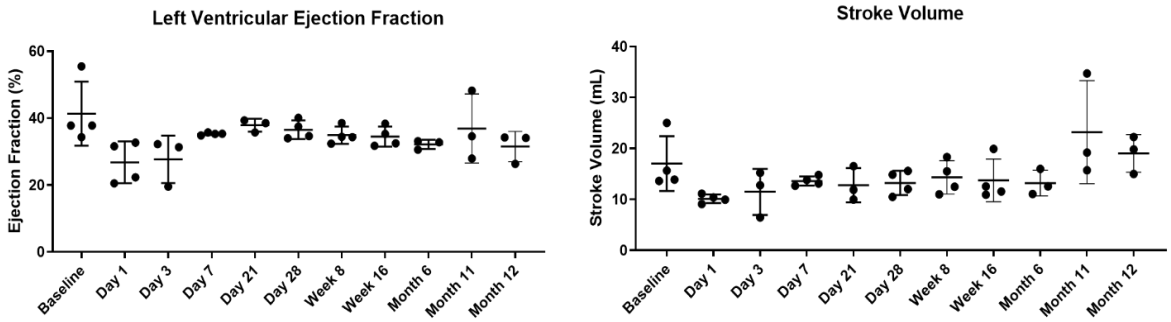

Supplemental Figure 6. LVEF and stroke volume do not change over time after surgical induction of myocardial infarction.

MR imaging was initiated at the beginning of the first PET scan (^{13}N-NH$_3$ or [^{18}F]LCE470) and continued throughout the full imaging session. MR sequences included short axis cine stacks of the left ventricle synchronized to the Echo signal (true fast imaging with steady-state free precession (TrueFISP), slice thickness of 6 mm, 356 x 216 voxels with voxel size of 1.09 x 1.09 mm, 10-12 second acquisition time, based in heart rate) with each slice acquired during a breath hold where the ventilator was manually turned off for 10 seconds to allow for image acquisition. T1 maps (Echo triggered modified Lock-Locker inversion recovery sequence, slice thickness 6 mm, 256 x 144 voxels, voxel size 1.09 x 1.09, 12 second acquisition time, based on heart rate) were generated in a single breath hold to acquire 2- and 4- chamber views (Siemens Work In

Progress). A commercial cardiovascular image analysis software Circle CVI42 (Circle Cardiovascular Imaging Inc, Calgary) was used to calculate the following parameters of heart function: left ventricular ejection fraction (EF), stroke volume (SV), end systolic and diastolic volume (ESV, EDV), and end systolic and diastolic mass (ESM, EDM). Short axis TrueFISP image series were uploaded and automated segmentation for systole and diastole were generated. Manual adjustments were made when needed to correct for LV segmentation and to select slices in the series at systole and diastole for calculating functional parameters. Slices in the series were excluded due to poor image quality, if the aorta or left atrium were visible, or if they were past the apex. Based on proper segmentation of the series, all cardiac function values were calculated automatically in the online software.

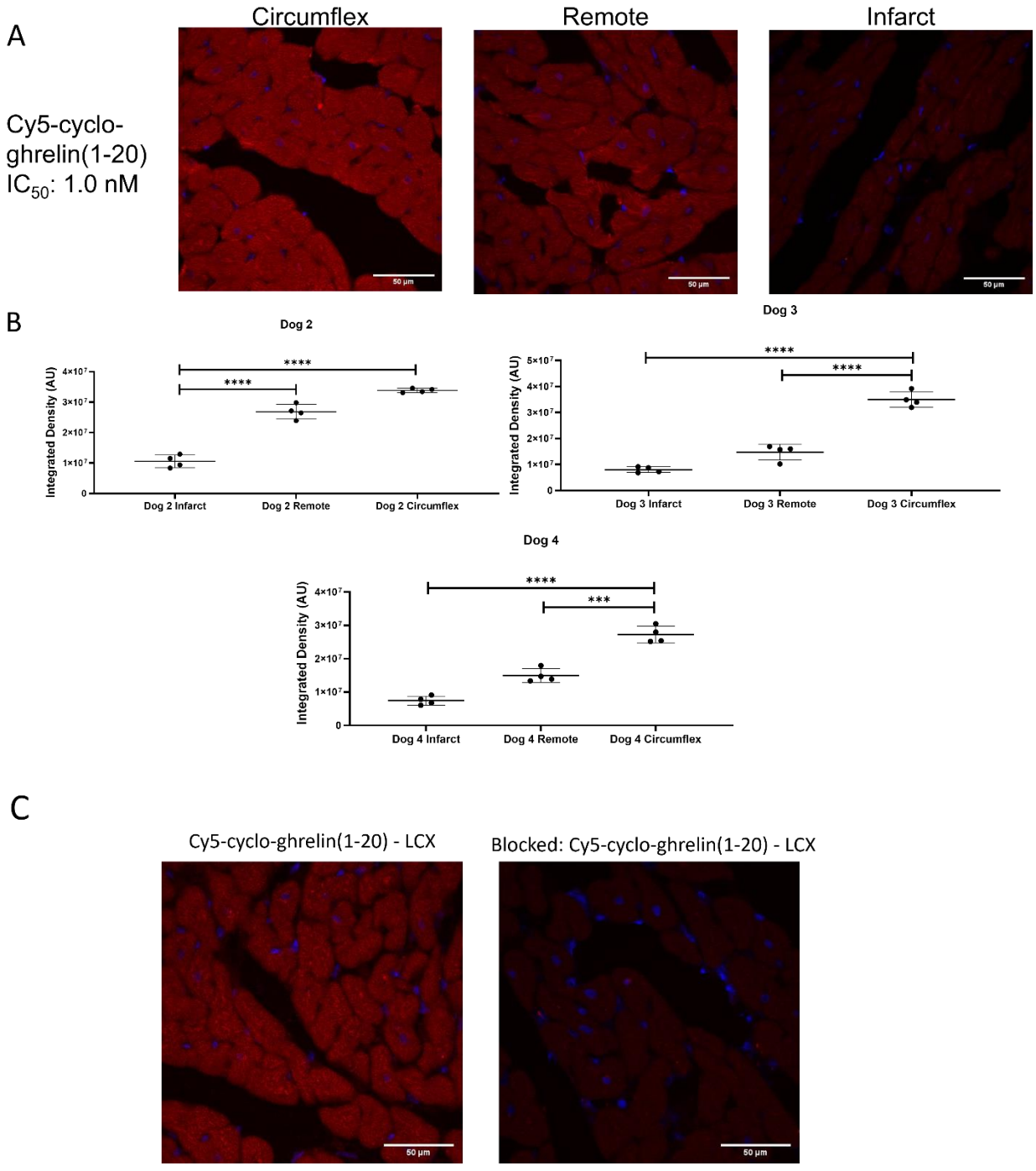

Supplemental Figure 7. Tissue Characterization of GHSR in Canine Heart. A) Representative fluorescence images of GHSR in the canine heart using Cy5-cyclo-ghrelin(1-20). DAPI nuclear stain is in blue. B) Quantification of fluorescent images for each dog (n=3) at end point. There are significant differences between infarct and remote, remote and circumflex.

(***p<0.001; ****p<0.0001) C) Blocking study showed a decrease in fluorescence signal in the LCX region in the presence of hexarelin. LCX: left circumflex tissue. At 1.5 years after MI, hounds were euthanized, and tissue was obtained for histological analysis. Immediately after euthanasia, the chest was opened and the entire heart was removed. Myocardial tissue samples (roughly 1 cm^3) were collected in duplicate from areas within the left ventricle that corresponded to the tissue ROIs selected for tracer uptake analysis, immediately snap frozen in liquid nitrogen and kept at -80°C until use. Frozen tissue blocks were embedded in optical cutting temperature medium (OCT) and left to freeze at -80°C overnight. Tissue was cryosectioned at 5-6 μm and adhered to positively charged microscope slides. Tissue sections were subsequently fixed using ice-cold acetone for 15 minutes at room temperature (RT) and incubated with the far-red fluorescent ghrelin analogue (cyclo 12,16)-[Dpr_3(octanoyl),Lys_{20}(SulfoCy5)] ghrelin(1-20)[14], termed Cy5-cyclo-ghrelin(1-20), at a 20 μM concentration for 1 hour at RT. We have previously used [Dpr^3(n-octanoyl),Lys^{19}(sulfo-Cy5)]ghrelin(1-19) to detect GHSR in human[8] and mouse cardiac tissue[7]. Cy5-cyclo-ghrelin (1-20) has a greatly improved affinity towards GHSR (1.0 nM)[14]. Samples were then incubated with 300 nM 4',6-diamidino-2-phenulindole (DAPI) to visualize nuclei, followed by mounting with ProLong Diamond Antifade (Life Technologies). High-resolution images were captured with a Nikon A1R Confocal Microscope at 60x magnification using an oil immersion lens. For each tissue location in the heart (technical replicate of 2), five random fields of view were captured with image acquisition parameters (exposure time, gain and LUT) set at the same values for all tissue sections. Fluorescence images were analyzed with FIJI v. 1.49v, a distribution of ImageJ software (National Institutes of Health) as we have done previously[7–9]. The Percentile algorithm within ImageJ was used to quantify Cy5 fluorescence intensity patterns corresponding to GHSR localization in tissue sections. The

integrated density represents the mean intensity of the positive signal above threshold in scaled units divided by the area in pixels.

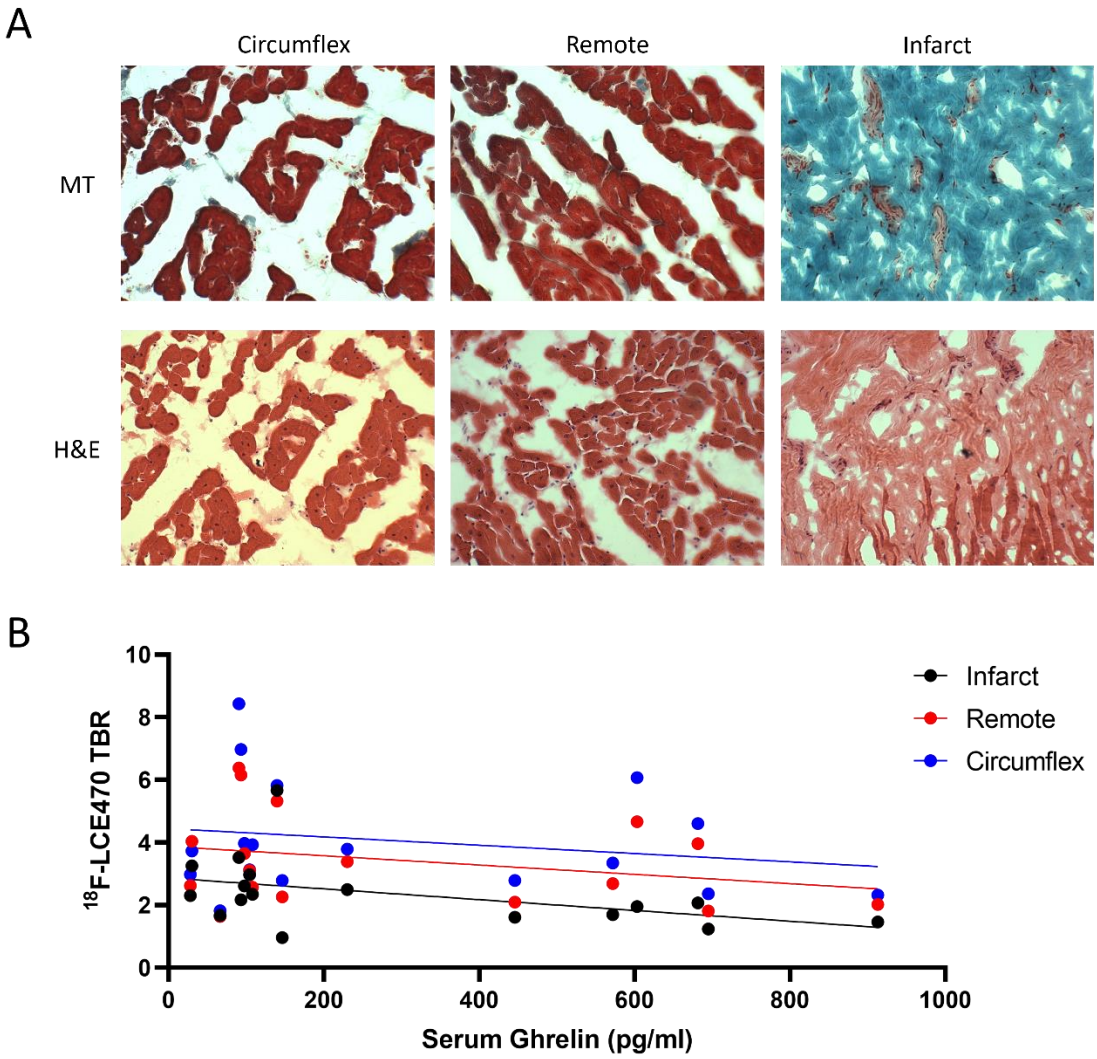

Supplemental Figure 8. Representative qualitative images of fibrosis and hematoxylin and eosin (H&E) are shown in each region.

A) Adjacent sections were stained with Masson's Trichrome and H&E by the Molecular Pathology Department at Robarts Research Institute. Images of all cardiac tissue sections that were collected from the hearts (infarct, edge of infarct, remote, left circumflex) were acquired

using bright field microscopy at 10X, 20X and 40X magnifications with a Zeiss Axioskope EL-Einsatz microscope and Northern Eclipse software. Masson's trichrome (MT) stained for fibrosis (blue) and non-fibrotic tissue (red) where there were significant amounts of fibrosis in the infarct compared to the remote and circumflex tissue regions (A top). H&E stain confirmed differences in tissue distribution and type as seen in fibrosis (A bottom).

B) To determine the impact of circulating ghrelin on [^{18}F]LCE470 tracer binding in the heart, plasma ghrelin levels were compared to [^{18}F]LCE470 TBR at all time points from baseline to 12 months post MI. Linear regression of plasma ghrelin and ^{18}F-LCE470 distribution volume were compared based on region (infarct, remote, circumflex). Blood plasma was obtained at all time points prior to imaging to evaluate circulating levels of ghrelin. Samples of whole blood were added to tubes containing a complete mini protease inhibitor (Sigma Aldrich) to inhibit degradation of active circulating biomarkers. The blood was centrifuged at 3000rpm for 10 min at 4°C to separate red blood cells from plasma. The plasma was collected and kept at -80°C until end of the study for analysis. Levels of canine ghrelin were measured using multiplexed immunoassay kits (CGTMAG-98K-02, Millipore Sigma) according to manufacturers' instructions (R&D Systems, Minneapolis, MN). A Bio-Plex 200 readout system was used (Bio-Rad), which utilizes Luminex® xMAP fluorescent bead-based technology (Luminex Corporation, Austin, TX). Levels were automatically calculated from standard curves using Bio-Plex Manager software (v. 6.1, Bio-Rad). Linear regression between LCE470 distribution volume and circulating plasma ghrelin levels based on region (infarct, remote, circumflex). There were no significant linear regressions in any region where circulating ghrelin did not alter the binding of LCE470 regionally in the heart

***Methods**:*

6-bromo-2-(2,4-difluorophenyl)-4H-benzo[d][1,3]oxazin-4-one (1)

The compound was made according to literature procedure. To a solution of 2-amino-5-bromobenzoic acid (5g, 23mmol) and triethylamine (10ml; 70mmol) in dichloromethane (50ml) was added 2,4-difluorobenzoyl chloride (4.9g, 28mmol) drop wise at room temperature. After the suspension was stirred for 12 hours, the solvent was removed and acetic acid anhydride (45ml) was added. The resulting suspension was stirred at 50oC for 2 hours. After cooling down, the precipitate was collected by filtration and washed with methanol (100ml). The product was dried under vacuum for an hour to give 6.6g light yellow powder with 85% yield. UP LC-MS (waters) method: 5-95% acetonitrile (0.1% TFA) in water (0.1% TFA), 3mins run; Calculated m/z 337.9628 (MH+), Found m/z: 337.9193; RT (min): 2.38.

(R)-tert-butyl 3-((5-bromo-2-(2,4-difluorobenzamido)benzamido)methyl)piperidine-1-carboxylate (2)

The compound was made according to literature procedure with some modifications. Compound 1 (3.7g, 10.98mmol) was dissolved in toluene (125ml). (R)-1-Boc-3-(aminomethyl)pyrrolidine (2.40 g, 11.21mmol) was added and it was refluxed at 110 °C for 8h. The reaction mixture was cooled down and solvent was removed. The precipitate was washed with hexane (50ml) to give pure product as light yellow power with 98% yield. UP LC-MS (waters) method: 5-95% acetonitrile (0.1% TFA) in water (0.1% TFA), 3mins run; Calculated m/z 552.1310(MH+), Found m/z: 552.1366; RT (min): 2.68.

(R)-tert-butyl 3-((5-bromo-2-(2,4-difluorobenzamido)benzamido)methyl)piperidine-1-carboxylate (3)

Compound 2 (1.50 g, 2.72 mmol) was added to microwave reaction vessel, followed by ethylene glycol (12 mL) and LiOH (0.13mg, 5.44 mmol). The resulting mixture was subjected to microwave irradiation with stirring for 30 minutes at 150°C, cooled to room temperature, and diluted with CH2Cl2 (50ml) and water (50ml). The organic layer was washed with brine (50 mL) twice. The combined organic layer was dried over Mg2SO4 and then concentrated under reduced pressure. The crude compound was purified via silica gel column chromatography using an elution of 50% ethyl acetate in hexanes to give 0.61g of the product as white foam with 38% yield. UP LC-MS (waters) method: 5-95% acetonitrile (0.1% TFA) in water (0.1% TFA), 3mins run; Calculated m/z 576.1509(MH+), Found m/z: 576.1633; RT (min): 2.34.

(S)-2-(2-fluoro-4-(2-hydroxyethoxy)phenyl)-6-((5-fluoropyridin-2-yl)oxy)-3-(piperidin-3-ylmethyl)quinazolin-4(3H)-one (4a)

Under a nitrogen atmosphere, compound 3 (623 mg, 1.08 mmol), copper(I) chloride (107 mg, 1.08 mmol), 2,2,6,6-tetramethylheptane-3,5-dione (TMHD) (100 mg, 0.54 mmol),5-fluoro-2-pyridinol (184 mg, 1.63 mmol) and Cs2CO3 (704 mg, 2.16 mmol) were added to 1-methyl-2-pyrrolidone (3 mL). The reaction mixture was stirred for 16 h at 115 °C, cooled, and passed through a Celite bed. The filtrate was diluted with DCM (50ml) and washed with brine (50 ml × 2). The organic layer was dried over Mg2SO4, filtered and concentrated under reduced pressure. The crude product was purified by reverse phase chromatography (Isolera One, HS-C18-30g cartridge) with a gradient from 0 to 70 % acetonitrile in water. The product was lyophilized to give 213 mg of the Boc-protected intermediate as white powder with 32% yield. UP LC-MS

(waters) method: 5-95% acetonitrile (0.1% TFA) in water (0.1% TFA), 3mins run; Calculated m/z: 609.2525 (MH+), Found m/z: 609.2766; RT (min): 2.18. The Boc-protected intermediate (70 mg, 0.12 mmol) was dissolved in CH2Cl2 (5 mL). TFA (1 mL) was added. The solution was stirred for 3 hours at room temperature. The solvent was removed and saturated aqueous NaHCO3 solution was added. The product was then extracted with EtOAc (2×). The combined organic layers were dried with Na2SO4 and filtered, and the solvent was removed under reduced pressure, and the crude compound was purified by reverse phase chromatography (Isolera One, HS-C18-30g cartridge) with a gradient from 05 to 60 % methanol in water. The product was lyophilized to yield 40 mg white powder with 66% yield. UP LC-MS (waters) method: 5-95% acetonitrile (0.1% TFA) in water (0.1% TFA), 3mins run, RT (min) 1.29, m/z 509.2; HRMS (ES+) for C27H27F2N4O4 (MH+), calcd 509.2000, found 509.2003. 1H NMR (400 MHz, methanol-d4) δ ppm 8.05 (d, J = 3.1 Hz, 1H), 7.91 (d, J = 2.7 Hz, 1H), 7.78 – 7.71 (m, 2H), 7.65 (dd, J = 8.9, 2.8 Hz, 1H), 7.57 (t, J = 8.4 Hz, 1H), 7.17 (dd, J = 9.0, 3.5 Hz, 1H), 7.05 – 6.97 (m, 2H), 4.38 – 4.03 (m, 3H), 4.02 – 3.66 (m, 3H), 3.26 – 3.14 (m, 2H), 2.92 – 2.75 (m, 1H), 2.75 – 2.52 (m, 1H), 2.14 – 2.01 (m, 1H), 1.92 – 1.77 (m, 1H), 1.67 – 1.48 (m, 2H), 1.27 – 1.10 (m, 1H). 19F NMR (3 76 MHz, methanol-d4) δ ppm -112.58 – -113.26 (m), -136.07 – -136.26 (m)

(S)-2-(2-fluoro-4-(2-hydroxyethoxy)phenyl)-6-(4-fluorophenoxy)-3-(piperidin-3-ylmethyl)quinazolin-4(3H)-one (4b)

The method similar for the preparation of compound 4a was used, except replacing 5-fluoro-2-pyridinol with 4-fluorophenol. The crude Boc-protected intermediate was purified via silica gel column chromatography using a elution of 30% ethyl acetate in hexanes to give 308 mg of the product with 61% yield. UP LC-MS (waters) method: 5-95% acetonitrile (0.1% TFA) in water

(0.1% TFA), 3mins run; Calculated m/z: 608.2572 (MH+), Found m/z: 609.2756; RT (min): 2.50. After Boc-deprotection, the final product was purified by reverse phase chromatography (Isolera One, HS-C18-30g cartridge) with a gradient from 05 to 60 % methanol in water. The product was lyophilized to yield 200mg white powder with 77% yield. UP LC-MS (waters) method: 5-95% acetonitrile (0.1% TFA) in water (0.1% TFA), 3mins run, RT (min): 1.61, Found m/z: 508.2. HRMS (ESI+) for C28H28F2N3O4 (MH+), calcd 508.2048, found 508.2046. 1H NMR (400 MHz, methanol-d4) δ ppm 7.72 (d, J = 8.8 Hz, 1H), 7.62 – 7.51 (m, 3H), 7.24 – 7.11 (m, 4H), 7.05 – 6.95 (m, 2H), 4.37 – 3.99 (m, 3H), 3.95 – 3.60 (m, 3H), 3.27 – 3.10 (m, 2H), 2.82 (t, J = 12.2 Hz, 1H), 2.74 – 2.53 (m, 1H), 2.10 – 1.98 (m, 1H), 1.89 – 1.76 (m, 1H), 1.69 – 1.43 (m, 2H), 1.28 – 1.05 (m, 1H). 19F NMR (376 MHz, methanol-d4) δ ppm -112.36 – -113.15 (m, 1F), -119.48 – -119.85 (m, 1F)

(S)-2-(2-fluoro-4-(2-hydroxyethoxy)phenyl)-6-((5-fluoropyridin-2-yl)oxy)-3-((1-isopropylpiperidin-3-yl)methyl)quinazolin-4(3H)-one (5a)

Compound 4a (127 mg, 0.25 mmol), 2-bromopropane (308 mg, 2.5 mmol), and K2CO3 (345 mg, 2.5 mmol) were combined in acetonitrile (5ml) and three drops of water was added and the resulting mixture was heated to 80 °C for 8 h. The solid was filtered off, and the filtrate was concentrated under reduced pressure. Saturated aqueous NaHCO3 solution was added, and the product was extracted with EtOAc (2×). The combined organic layers were dried with Na2SO4 and filtered. The solvent was removed under reduced pressure, and the crude product was purified by reverse phase chromatography (Isolera One, HS-C18-30g cartridge) with a gradient from 05 to 90 % methanol in water. The product was lyophilized to yield 100 mg white powder with 73% yield. UP LC-MS (waters) method: 5-95% acetonitrile (0.1% TFA) in water (0.1%

TFA), 3mins run, RT (min): 1.38, Found m/z: 551.3. HRMS (ESI+) for C30H33F2N4O4 (MH+), calcd 551.2470, found 551.2464. 1H NMR (400 MHz, methanol-d4) δ ppm 8.05 (d, J = 3.1 Hz, 1H), 7.92 (d, J = 2.7 Hz, 1H), 7.79 – 7.71 (m, 2H), 7.65 (dd, J = 8.8, 2.7 Hz, 1H), 7.58 (t, J = 8.4 Hz, 1H), 7.17 (dd, J = 9.0, 3.6 Hz, 1H), 7.05 – 6.97 (m, 2H), 4.31 – 4.09 (m, 3H), 3.96 – 3.71 (m, 3H), 3.50 – 3.39 (m, 1H), 3.28 – 3.16 (m, 1H), 2.91 – 2.60 (m, 2H), 2.31 – 2.13 (m, 1H), 2.01 – 1.86 (m, 1H), 1.71 – 1.49 (m, 2H), 1.37 – 1.00 (m, 8H). 19F NMR (376 MHz, methanol-d4) δ ppm -112.28 – -113.79 (m, 1F), -136.06 – -136.64 (m, 1F)

(S)-2-(2-fluoro-4-(2-hydroxyethoxy)phenyl)-6-(4-fluorophenoxy)-3-((1-isopropylpiperidin-3-yl)methyl)quinazolin-4(3H)-one(5b)

The method similar for the preparation of compound 5a was used, except compound 4a with 4b. The crude product was purified by reverse phase chromatography (Isolera One, HS-C18-30g cartridge) with a gradient elution from 05 to 90 % methanol (0.1% TFA) in water (0.1%TFA). The product was lyophilized to yield white powder with 70% yield. UP LC-MS (waters) method: 05-95% acetonitrile (0.1% TFA) in water (0.1% TFA), 3mins run, RT (min) 1.65, m/z: 550.3; HRMS (ESI+) for C31H34F2N3O4 (MH+), calcd 550.2517; found 550.2502. 1H NMR (400 MHz, methanol-d4) δ ppm 7.73 (d, J = 8.8 Hz, 1H), 7.62 – 7.52 (m, 3H), 7.24 – 7.12 (m, 4H), 7.07 – 6.96 (m, 2H), 4.30 – 4.01 (m, 3H), 3.95 – 3.68 (m, 3H), 3.49 – 3.39 (m, 1H), 3.28 – 3.14 (m, 1H), 2.88 – 2.57 (m, 2H), 2.25 – 2.12 (m, 1H), 1.96 – 1.83 (m, 1H), 1.68 – 1.37 (m, 2H), 1.34 – 0.91 (m, 8H). 19F NMR (376 MHz, methanol) δ ppm -112.52 – -113.48 (m, 1F), -119.91 – -120.02 (M, 1F)

(S)-2-(3-fluoro-4-(6-((5-fluoropyridin-2-yl)oxy)-3-((1-isopropylpiperidin-3-yl)methyl)-4-oxo-3,4-dihydroquinazolin-2-yl)phenoxy)ethyl 4-methylbenzenesulfonate (6a)

To a solution of p-Toluenesulfonic anhydride (95 mg, 0.29 mmol) in dry dichloromethane (3ml) was added Ytterbium(III) trifluoromethanesulfonate (Yb(OTf)3) (93 mg, 0.15 mmol) and the suspension was stirred for five minutes until most of the solid was dissolved. Compound 5a (80mg, 0.15 mmol) was added and the resulting mixture was subjected to microwave irradiation with stirring for one hour at 90 °C, cooled to room temperature and passed through a celite bed. The crude product was purified by reverse phase chromatography (Isolera One, HS-C18-30g cartridge) with a gradient elution from 20 to 80 % methanol (0.1% TFA) in water (0.1%TFA). The product was lyophilized to yield 100mg of white powder with 95% yield. UP LC-MS (waters) method: 05-95% acetonitrile (0.1% TFA) in water (0.1% TFA), 3mins run; Calculated m/z: 705.2558 (MH+), Found m/z: 705.2344; RT (min): 1.96. 1H NMR (400 MHz, methanol-d4) δ ppm 8.04 (d, J = 3.0 Hz, 1H), 7.91 (d, J = 2.7 Hz, 1H), 7.81 (d, J = 8.3 Hz, 2H), 7.78 – 7.69 (m, 2H), 7.64 (dd, J = 8.9, 2.7 Hz, 1H), 7.57 (t, J = 8.3 Hz, 1H), 7.47 (d, J = 8.3 Hz, 2H), 7.16 (dd, J = 8.9, 3.5 Hz, 1H), 6.97 – 6.86 (m, 2H), 4.44 – 4.35 (m, 2H), 4.33 – 4.27 (m, 2H), 4.28 – 4.05 (m, 1H), 3.94 – 3.66 (m, 1H), 3.49 – 3.37 (m, 1H), 3.27 – 3.13 (m, 1H), 2.87 – 2.59 (m, 2H), 2.47 (s, 3H), 2.29 – 2.12 (m, 1H), 1.99 – 1.81 (m, 1H), 1.70 – 1.47 (m, 2H), 1.37 – 1.00 (m, 8H). 19F NMR (376 MHz, methanol- d4) δ ppm -111.80 – -113.41(m, 1F), -133.11 – -136.25(m, 1F)

(S)-2-(3-fluoro-4-(6-(4-fluorophenoxy)-3-((1-isopropylpiperidin-3-yl)methyl)-4-oxo-3,4-dihydroquinazolin-2-yl)phenoxy)ethyl 4-methylbenzenesulfonate (6b)

The method similar for the preparation of compound 6a was used, except replacing compound 5a with 5b. The crude product was purified by reverse phase chromatography (Isolera One, HS-C18-30g cartridge) with a gradient elution from 20 to 80 % methanol (0.1% TFA) in water (0.1%TFA). The product was lyophilized to yield white powder with 75% yield. UP LC-MS (waters) method: 05-95% acetonitrile (0.1% TFA) in water (0.1% TFA), 3mins run; Calculated m/z: 704.2606 (MH+), Found m/z: 704.2416; RT (min): 2.11. 1H NMR (400 MHz, methanol-d4) δ ppm 7.81 (d, J = 8.3 Hz, 2H), 7.73 (d, J = 8.8 Hz, 1H), 7.62 – 7.52 (m, 3H), 7.47 (d, J = 8.0 Hz, 2H), 7.20 (s, 4H), 6.96 – 6.87 (m, 2H), 4.42 – 4.37 (m, 2H), 4.33 – 4.27 (m, 2H), 4.27 – 4.05 (m, 1H), 3.94 – 3.64 (m, 1H), 3.49 – 3.36 (m, 1H), 3.27 – 3.11 (m, 1H), 2.86 – 2.76 (m, 1H), 2.74 – 2.56 (m, 1H), 2.47 (s, 3H), 2.26 – 2.11 (m, 1H), 1.97 – 1.85 (m, 1H), 1.66 – 1.44 (m, 2H), 1.43 – 0.89 (m, 7H). 19F NMR (376 MHz, methanol- d4) δ ppm -112.65 – -113.59 (m, 1F), -120.27 – -120.38 (m, 1F)

(S)-2-(2-fluoro-4-(2-fluoroethoxy)phenyl)-6-((5-fluoropyridin-2-yl)oxy)-3-((1-isopropylpiperidin-3-yl)methyl)quinazolin-4(3H)-one (7a)

Tetrabutylammonium fluoride (45mg, 0.17mmol) was added into compound 6a (60 mg, 0.09mmol) in acetonitrile (3ml). The solution was stirred at 90oC for 3 hours. The solvent was removed under reduced pressure. Dichloromethane was added and washed with saturated NaHCO3. The organic layer was dried over Mg2SO4 and filtered. The crude product was purified by reverse phase chromatography (Isolera One, HS-C18-30g cartridge) with a gradient elution from 20 to 60 % methanol (0.1% TFA) in water (0.1%TFA). The product was lyophilized to yield 12 mg of white powder with 26% yield. UP LC-MS (waters) method: 05-95% acetonitrile (0.1% TFA) in water (0.1% TFA), 3mins run, RT (min): 1.64, Found m/z: 553.2.

HRMS (ESI+) for C30H32F3N4O3 (MH+), calcd 553.2427, found 553.2438. 1H NMR (400 MHz, methanol- d4) δ ppm 8.05 (d, J = 3.1 Hz, 1H), 7.92 (d, J = 2.7 Hz, 1H), 7.78 – 7.71 (m, 2H), 7.65 (dd, J = 8.8, 2.7 Hz, 1H), 7.60 (t, J = 8.8 Hz, 1H), 7.17 (d, J = 9.0 Hz, 1H), 7.07 – 7.00 (m, 2H), 4.85 – 4.81 (m, 1H), 4.73 – 4.70 (m, 1H), 4.40 – 4.36 (m, 1H), 4.32 – 4.29 (m, 1H), 4.28 – 4.07 (m, 1H), 3.99 – 3.72 (m, 1H), 3.49 – 3.40 (m, 1H), 3.27 – 3.12 (m, 1H), 2.91 – 2.61 (m, 2H), 2.29 – 2.15 (m, 1H), 1.97 – 1.88 (m, 1H), 1.70 – 1.51 (m, 2H), 1.38 – 1.03 (m, 8H). 19F NMR (376 MHz, methanol- d4) δ -112.33 – -113.44 (m, 1F), -136.23 – -136.47 (m, 1F), -224.60 – -225.32 (m, 1F)

(S)-2-(2-fluoro-4-(2-fluoroethoxy)phenyl)-6-(4-fluorophenoxy)-3-((1-isopropylpiperidin-3-yl)methyl)quinazolin-4(3H)-one (7b)

The method similar for the preparation of compound 7a was used. The crude product was purified by reverse phase chromatography (Isolera One, HS-C18-30g cartridge) with a gradient elution from 5 to 80 % methanol (0.1% TFA) in water (0.1%TFA). The product was lyophilized to yield white powder with 33% yield. UP LC-MS (waters) method: 05-95% acetonitrile (0.1% TFA) in water (0.1% TFA), 3mins run, RT (min): 1.86, Found m/z: 552.3. HRMS (ESI+) for C31H33F3N3O3 (MH+), calcd 552.2474, found 552.2471. 1H NMR (400 MHz, methanol- d4) δ ppm 7.73 (d, J = 8.7 Hz, 1H), 7.64 – 7.55 (m, 3H), 7.24 – 7.12 (m, 4H), 7.02 (t, J = 8.7 Hz, 2H), 4.84 – 4.78 (m, 1H), 4.73 – 4.65 (m, 1H), 4.40 – 4.33 (m, 1H), 4.33 – 4.28 (m, 1H), 4.28 – 4.04 (m, 1H), 3.95 – 3.67 (m, 1H), 3.49 – 3.36 (m, 1H), 3.26 – 3.11 (m, 1H), 2.89 – 2.58 (m, 2H), 2.23 (s, 1H), 1.98 – 1.84 (m, 1H), 1.68 – 1.46 (m, 2H), 1.36 – 0.99 (m, 8H). 19F NMR (376 MHz, methanol- d4) δ ppm -112.24 – -113.04 (m, 1F), -119.47 – -120.05 (m, 1F), -224.61 – -225.31 (m, 1F)

Radiochemistry

Production of [^{18}F]Fluoride

The [^{18}F-]anion was produced by the PET cyclotron (St. Joseph's Health Care London Ontario, Canada) as a result of the 18O(p,n)18F reaction involving proton bombardment of [^{18}O]H_2O. A Waters Sep-Pak® Accell™ PlusLight (46 mg) QMA Carbonate cartridge was pre-activated by slowly treating with EtOH (10 ml) and Milli-Q® water (10 ml) and then flushing with air. The radioactive [^{18}F-] anion was then trapped by drawing up the [^{18}O]H_2O solution containing it through the Sep-Pak.

Synthesis of [^{18}F]7b

To potassium carbonate (3.0 mg) and Kryptofix 222 (10.0 mg) was added water (200 μl) and MeCN (800 μl) and the resulting solution used to elute the Sep-Pak® containing [^{18}F]fluoride into a glass vial. The mixture was dried azeotropically (120 °C). The drying step was repeated twice more after the drop-wise addition of anhydrous MeCN (1 ml). 16b (2.0 mg in 0.5 mL of MeCN) was added to the aforementioned mixture, and the mixture was heated at 100°C for 10 min under sealed conditions. 0.5ml of water containing 0.1% TFA was added. The radiolabelled compound was purified by semi-preparative HPLC using 40-80% MeCN in Water (0.1% TFA, flow rate: 4.5ml/min, 15min run, 2min wash).

Radioligand binding assay

The affinity for GHS-R1a was determined using a radioligand binding assay. Assays were performed using GHS-R1a transfected HEK293 cells as the receptor source and human [^{125}I-

His9]ghrelin(1-28) (PerkinElmer Inc.) as the radioligand. Human ghrelin(1-28) (purchased from Abcam) was used as a reference to ensure the validity of the results. Test peptides (at concentrations of 10^{-5}M, 10^{-6}M, 10^{-7}M, 10^{-8}M, 10^{-9}M, 10^{-10}M and 10^{-11}M) and [^{125}I-His9]ghrelin (15 pM per assay tube) were mixed in binding buffer (25 mM HEPES, 5 mM magnesium chloride, 1 mM calcium chloride, 2.5 mM EDTA, and 0.4% BSA, pH 7.4). The HEK293 cells (50,000 cells per assay tube) was added to the assay tube containing test peptides and [^{125}I]-ghrelin. The resulting suspension was incubated for 20 min with shaking (550 rpm). Unbound [^{125}I]-ghrelin was washed off and the amount of [^{125}I-His9]ghrelin bound to GHS-R1a was measured by a Gamma counter (cobra II auto gamma counter/Perkin Elmer). All binding assays were performed in triplicate.

Appendix A: U-HPLC Chromatograms and Purities

Compds.	Purity (%)
4a	97
4b	99
5a	97
5b	99
7a	99
7b	98

UHPLC Chromatograms

4a

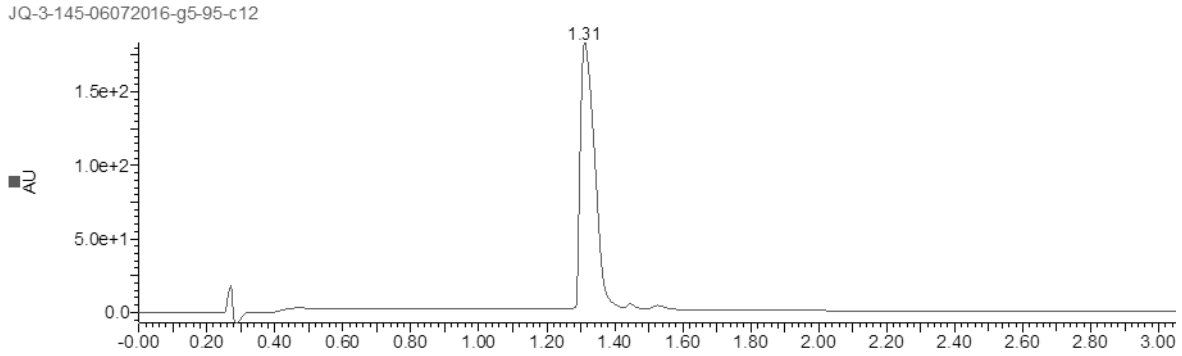

4b

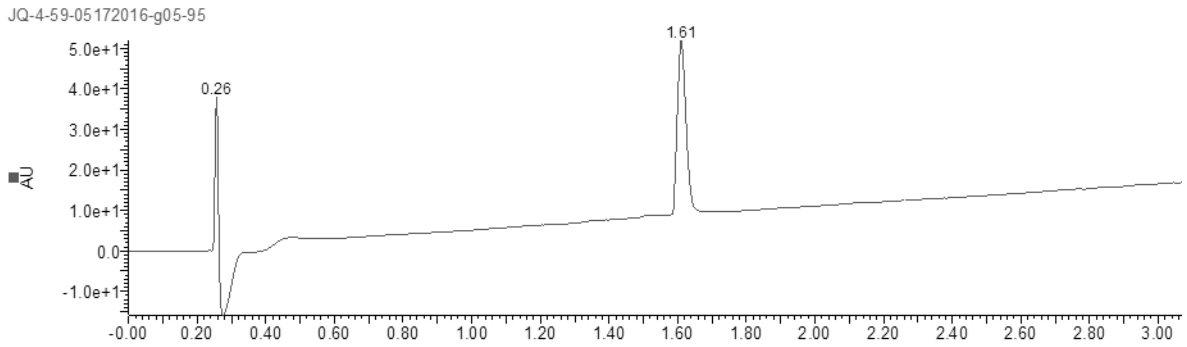

5a

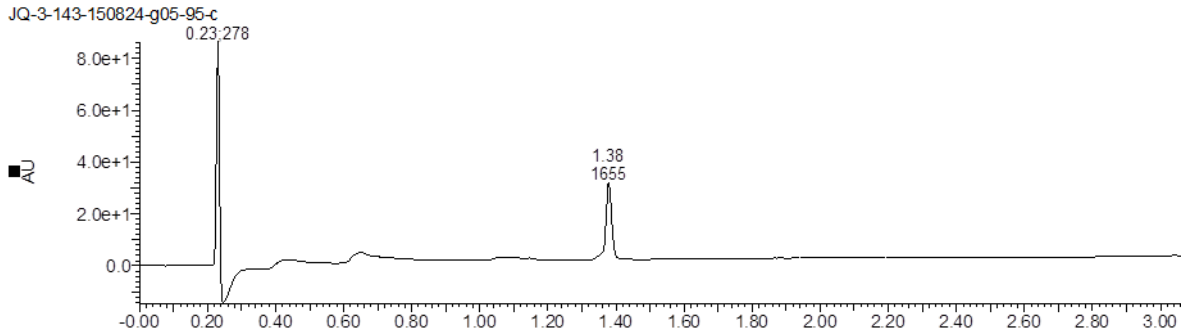
JQ-3-143-150824-g05-95-c
0.23;278
1.38
1655
AU
8.0e+1
6.0e+1
4.0e+1
2.0e+1
0.0
-0.00
0.20
0.40
0.60
0.80
1.00
1.20
1.40
1.60
1.80
2.00
2.20
2.40
2.60
2.80
3.00

5b

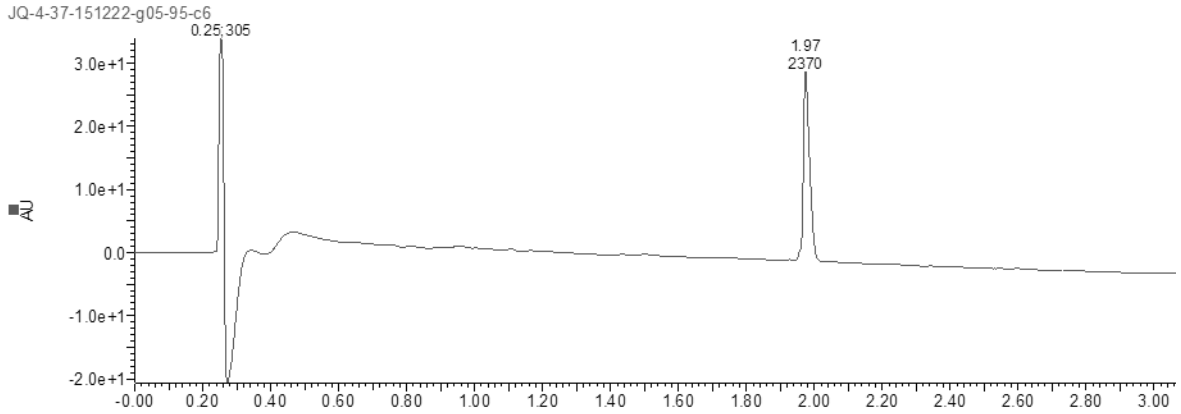
JQ-4-37-151222-g05-95-c6
0.25;305
1.97
2370
AU
3.0e+1
2.0e+1
1.0e+1
0.0
-1.0e+1
-2.0e+1
-0.00
0.20
0.40
0.60
0.80
1.00
1.20
1.40
1.60
1.80
2.00
2.20
2.40
2.60
2.80
3.00

7a

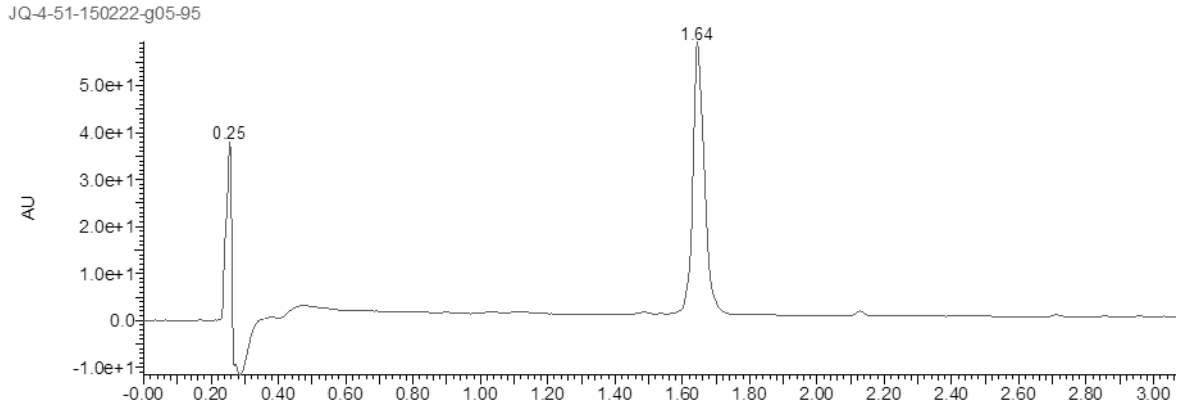
JQ-4-51-150222-g05-95
1.64
0.25
AU
5.0e+1
4.0e+1
3.0e+1
2.0e+1
1.0e+1
0.0
-1.0e+1
-0.00 0.20 0.40 0.60 0.80 1.00 1.20 1.40 1.60 1.80 2.00 2.20 2.40 2.60 2.80 3.00

7b

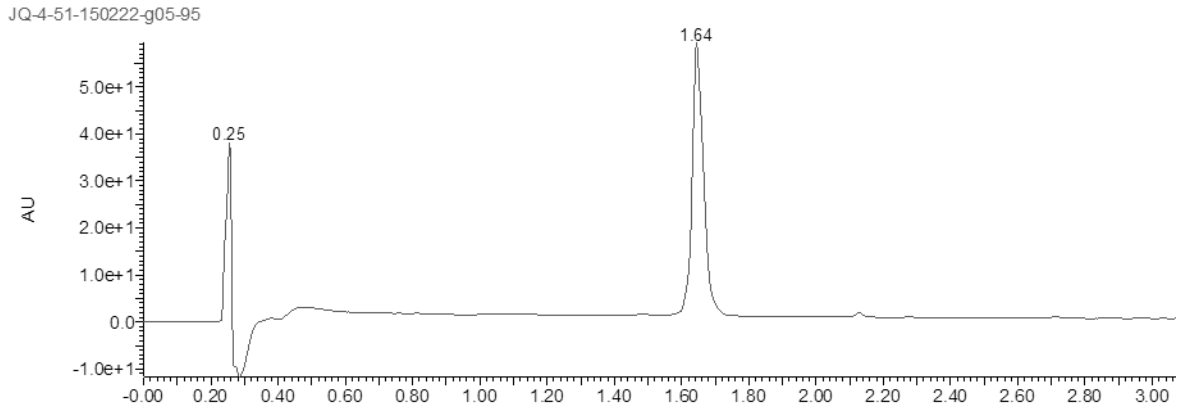
JQ-4-51-150222-g05-95
1.64
0.25
AU
5.0e+1
4.0e+1
3.0e+1
2.0e+1
1.0e+1
0.0
-1.0e+1
-0.00 0.20 0.40 0.60 0.80 1.00 1.20 1.40 1.60 1.80 2.00 2.20 2.40 2.60 2.80 3.00

Appendix B: ^{1}H and ^{19}F NMR spectra

4a

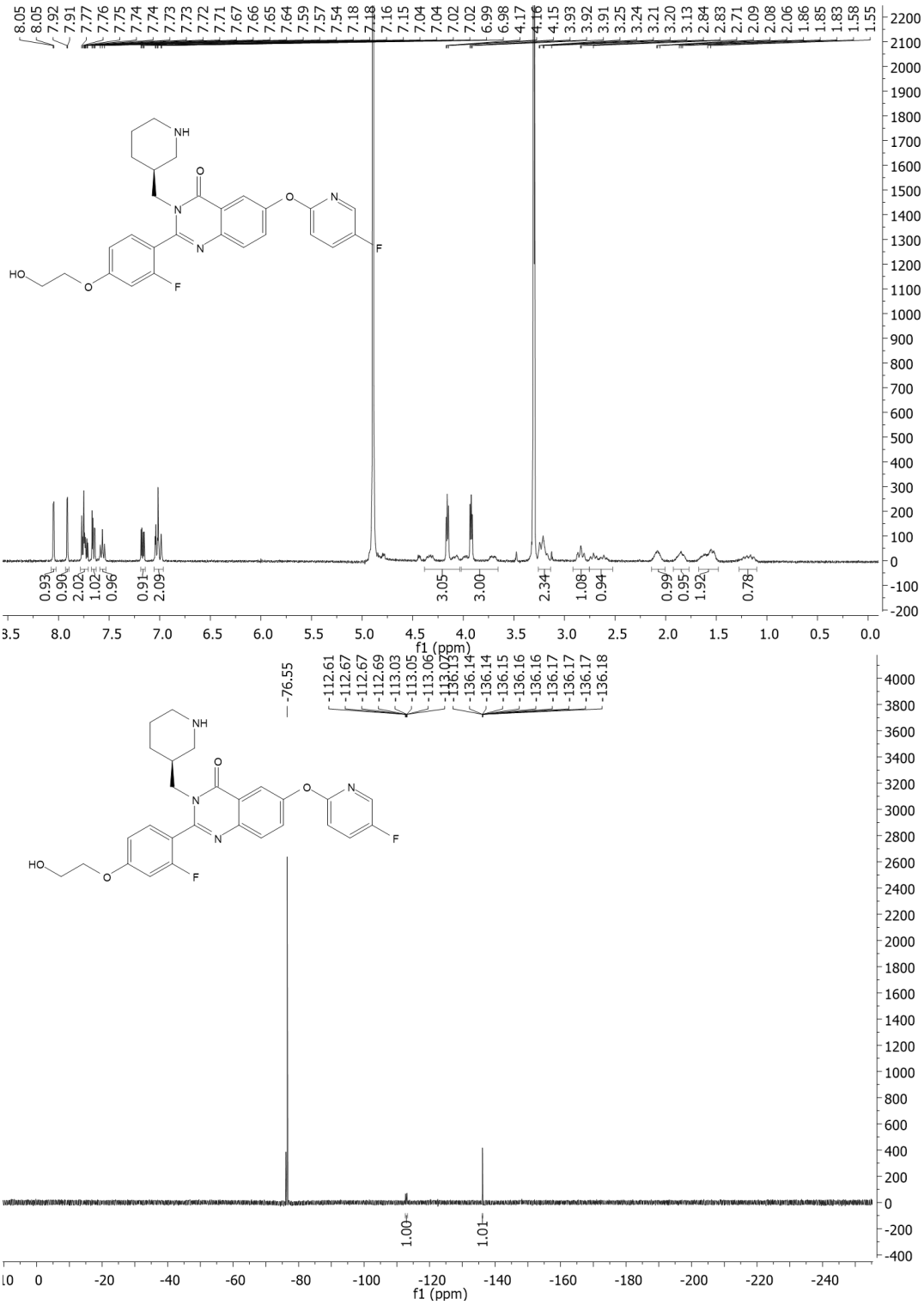

4b

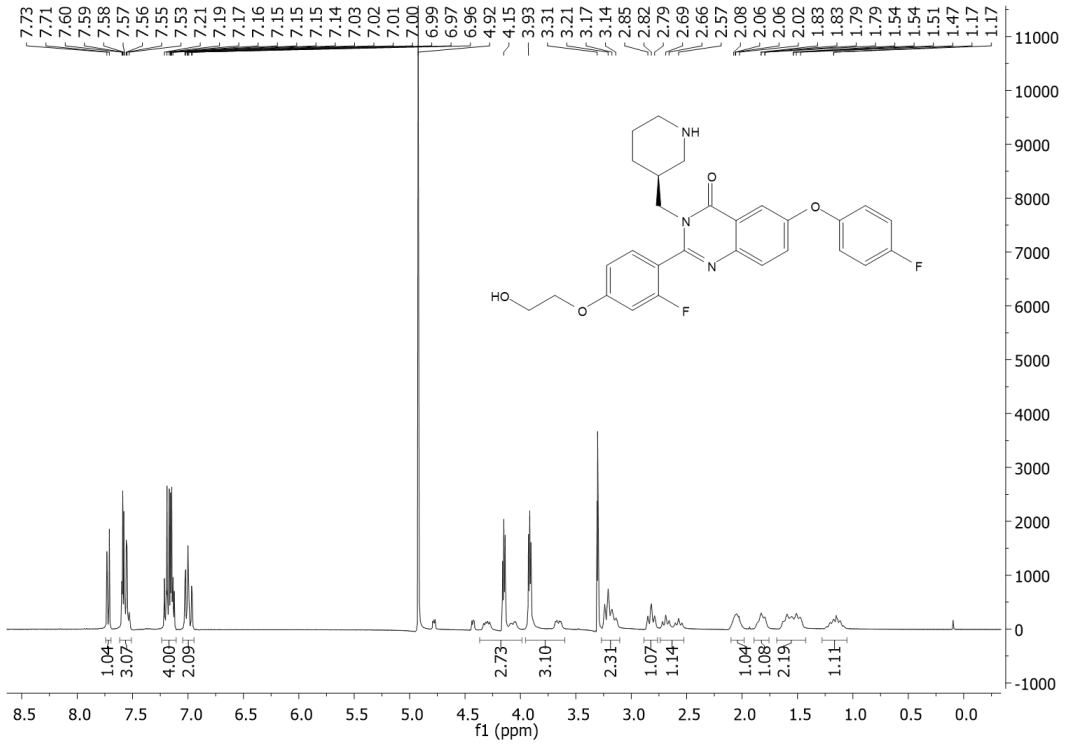
7.73 7.71 7.60 7.59 7.58 7.57 7.56 7.55 7.53 7.21 7.19 7.17 7.16 7.15 7.15 7.15 7.14 7.03 7.02 7.01 7.00 6.99 6.97 6.96 4.92 4.15 3.93 3.31 3.21 3.17 3.14 2.85 2.82 2.79 2.69 2.66 2.57 2.08 2.06 2.06 2.02 1.83 1.79 1.79 1.54 1.54 1.51 1.47 1.17 1.17
NH
O
N
N
O
F
HO
O
F
1.04 3.07 4.00 2.09 2.73 3.10 2.31 1.07 1.14 1.04 1.08 2.19 1.11
f1 (ppm)

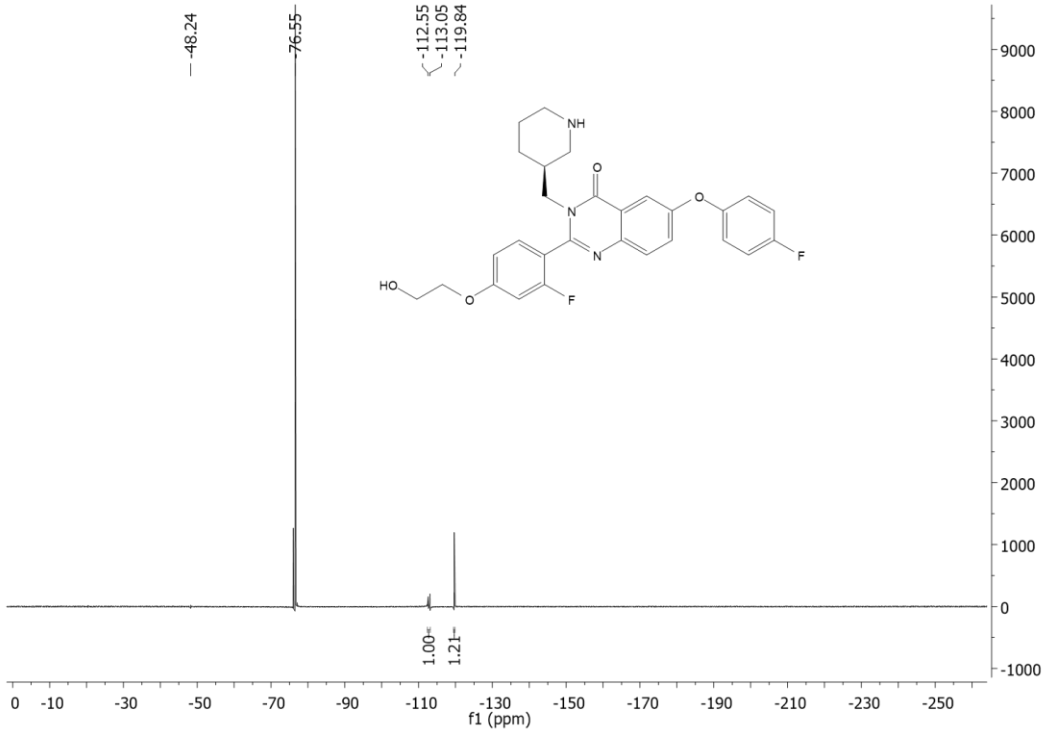
48.24
76.55
112.55
113.05
119.84
NH
O
N
N
O
F
HO
O
F
1.00 1.21
f1 (ppm)

5a

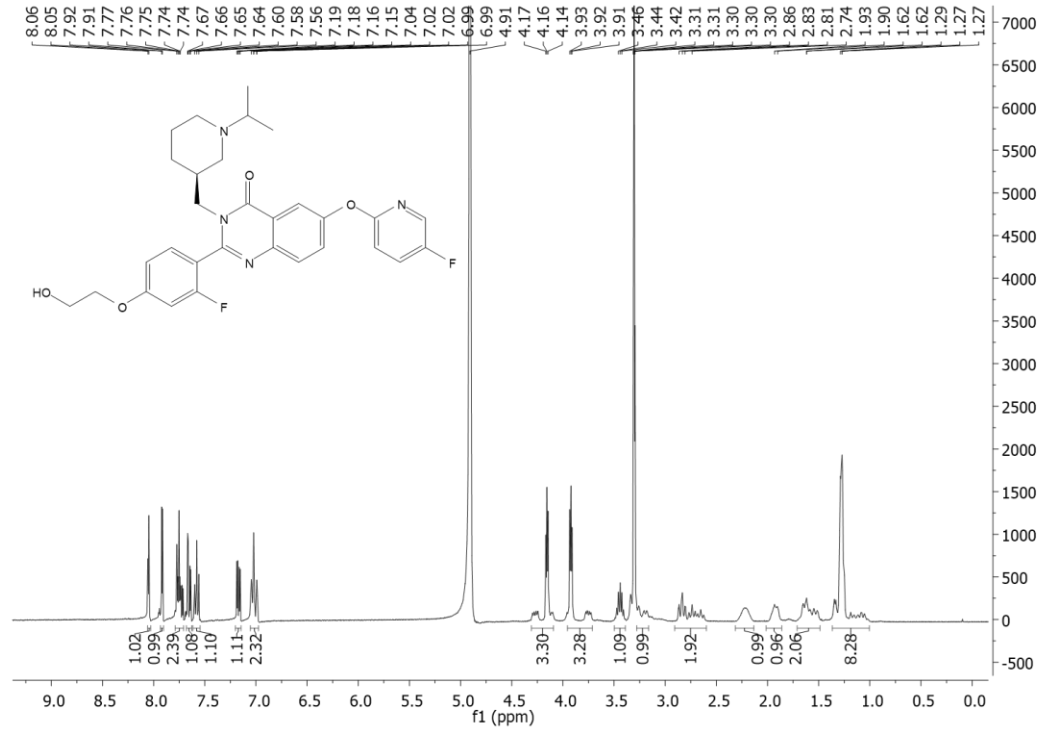
8.06 8.05 7.92 7.91 7.77 7.76 7.75 7.74 7.74 7.67 7.66 7.65 7.64 7.60 7.58 7.56 7.19 7.18 7.16 7.15 7.04 7.02 7.02 6.99 6.99 4.91 4.17 4.16 4.14 3.93 3.92 3.91 3.46 3.44 3.42 3.31 3.31 3.30 3.30 3.30 2.86 2.83 2.81 2.74 1.93 1.90 1.62 1.62 1.29 1.27 1.27
1.02 0.99 2.39 1.08 1.10 1.11 2.32 3.30 3.28 1.09 0.99 1.92 0.99 0.96 2.06 8.28
f1 (ppm)

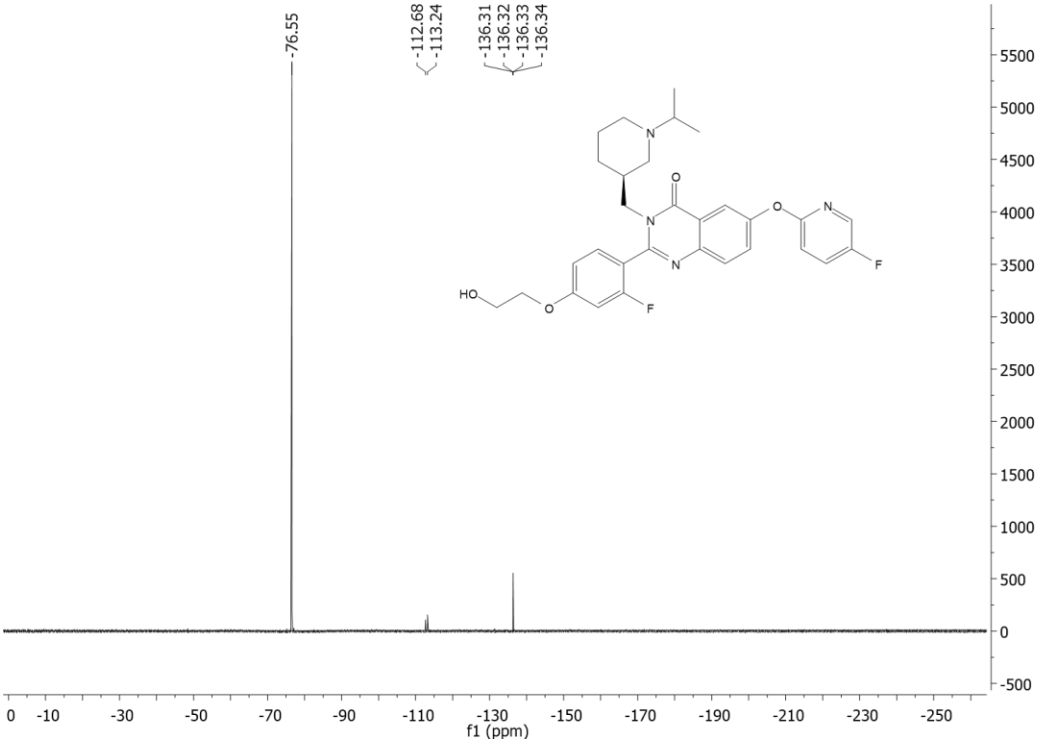
-76.55
-112.68
-113.24
-136.31
-136.32
-136.33
-136.34
f1 (ppm)

5b

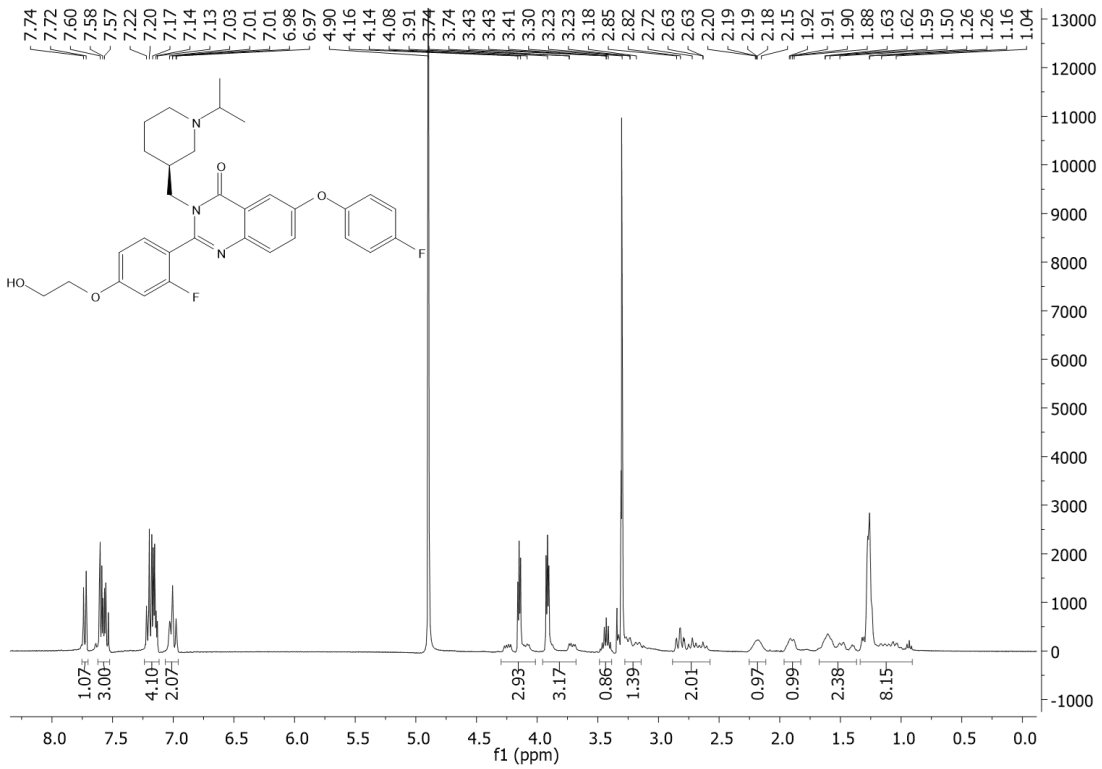
7.74 7.72 7.60 7.58 7.57 7.22 7.20 7.17 7.14 7.13 7.03 7.01 7.01 6.98 6.97 4.90 4.16 4.14 4.08 3.91 3.74 3.74 3.43 3.43 3.41 3.30 3.23 3.23 3.18 2.85 2.82 2.72 2.63 2.63 2.20 2.19 2.19 2.18 2.15 1.92 1.91 1.90 1.88 1.63 1.62 1.59 1.50 1.26 1.26 1.16 1.04
1.07 3.00 4.10 2.07 2.93 3.17 0.86 1.39 2.01 0.97 0.99 2.38 8.15
f1 (ppm)

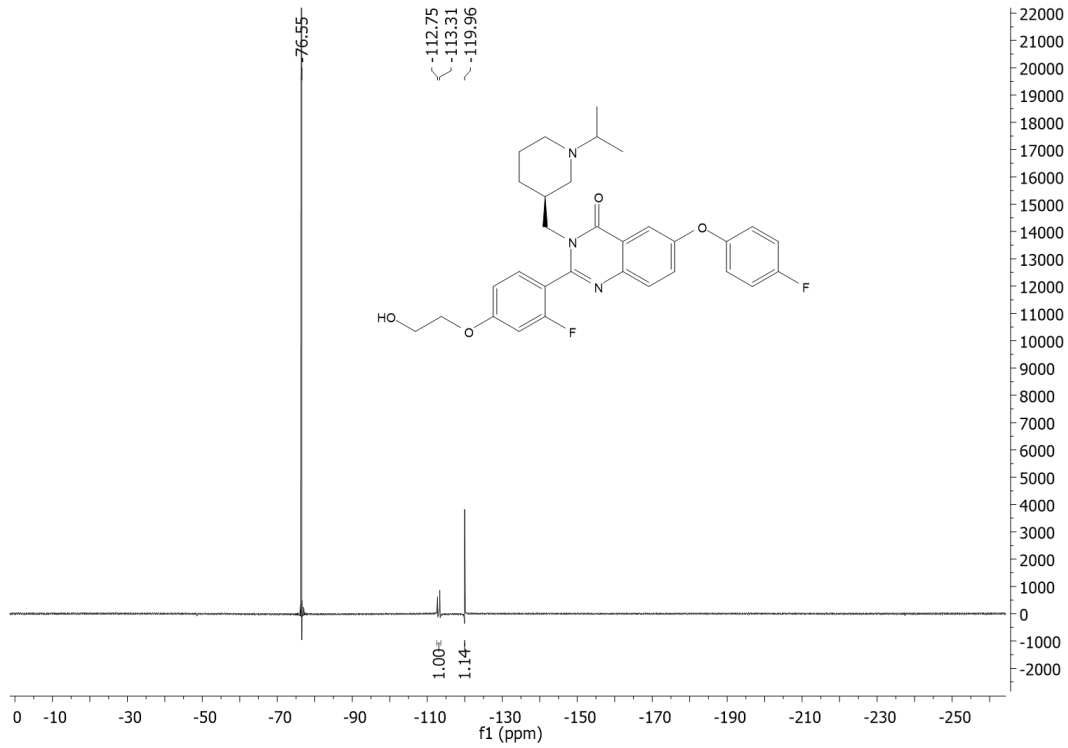
-76.55
-112.75
-113.31
-119.96
1.00 1.14
f1 (ppm)

6a

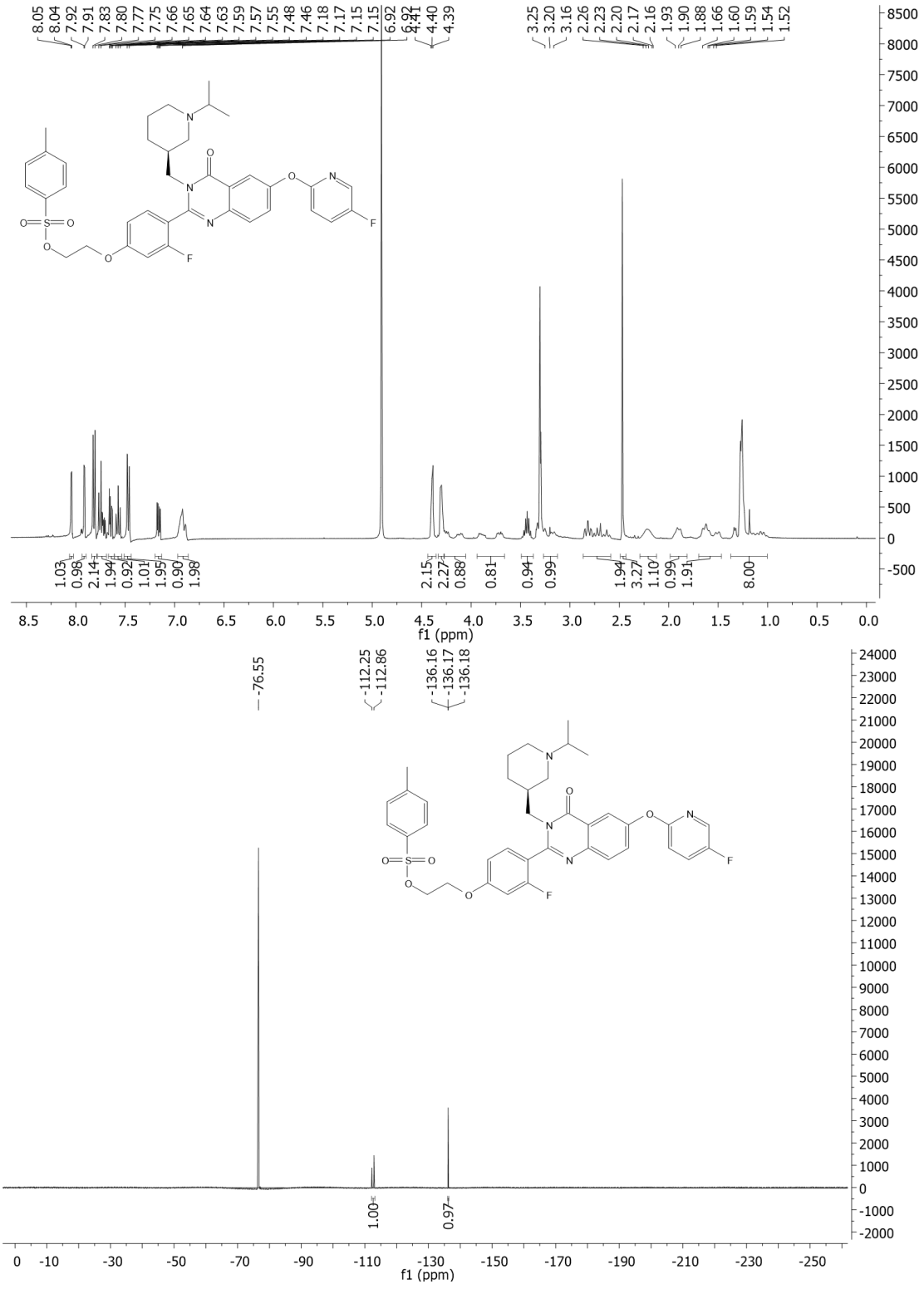
8.05
8.04
7.92
7.91
7.83
7.80
7.77
7.75
7.66
7.65
7.64
7.63
7.59
7.57
7.55
7.48
7.46
7.18
7.17
7.15
7.15
6.92
4.41
4.40
4.39
3.25
3.20
3.16
2.26
2.23
2.20
2.17
2.16
1.93
1.90
1.88
1.66
1.60
1.59
1.54
1.52
1.03
0.98
2.14
1.94
0.92
1.01
1.95
0.90
1.98
2.15
2.27
0.88
0.81
0.94
0.99
1.94
3.27
1.10
0.99
1.91
8.00
f1 (ppm)
-76.55
-112.25
-112.86
-136.16
-136.17
-136.18
1.00
0.97
f1 (ppm)

6b

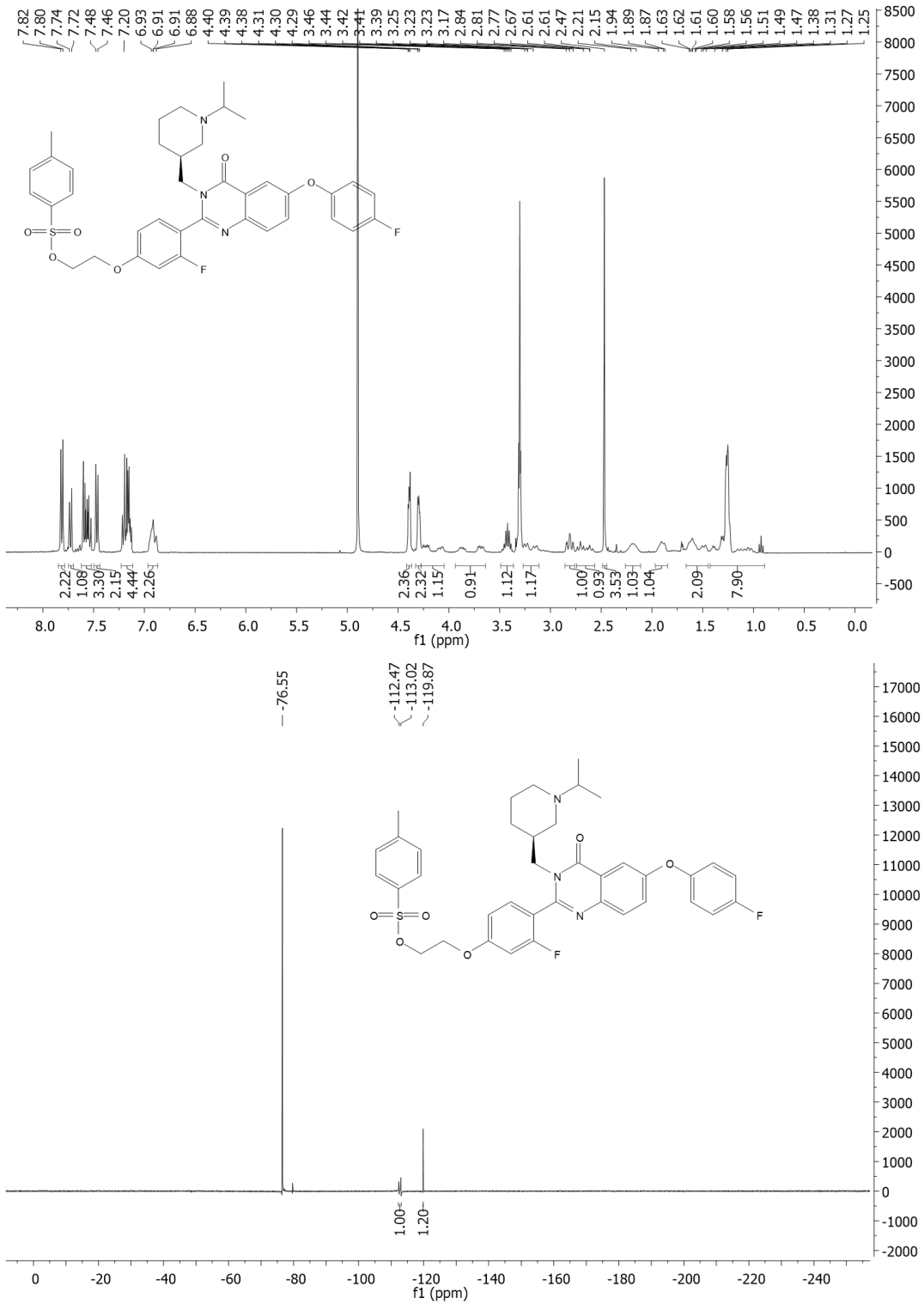
7.82 7.80 7.74 7.72 7.48 7.46 7.20 6.93 6.91 6.91 6.88 4.40 4.39 4.38 4.31 4.30 4.29 3.46 3.44 3.42 3.41 3.39 3.25 3.23 3.23 3.17 2.84 2.81 2.77 2.67 2.61 2.61 2.47 2.21 2.15 1.94 1.89 1.87 1.63 1.62 1.61 1.60 1.58 1.56 1.51 1.49 1.47 1.38 1.31 1.27 1.25
2.22 1.08 3.30 2.15 4.44 2.26 2.36 2.32 1.15 0.91 1.12 1.17 1.00 0.93 3.53 1.03 1.04 2.09 7.90
f1 (ppm)
-76.55 -112.47 -113.02 -119.87
1.00 1.20
f1 (ppm)

7a

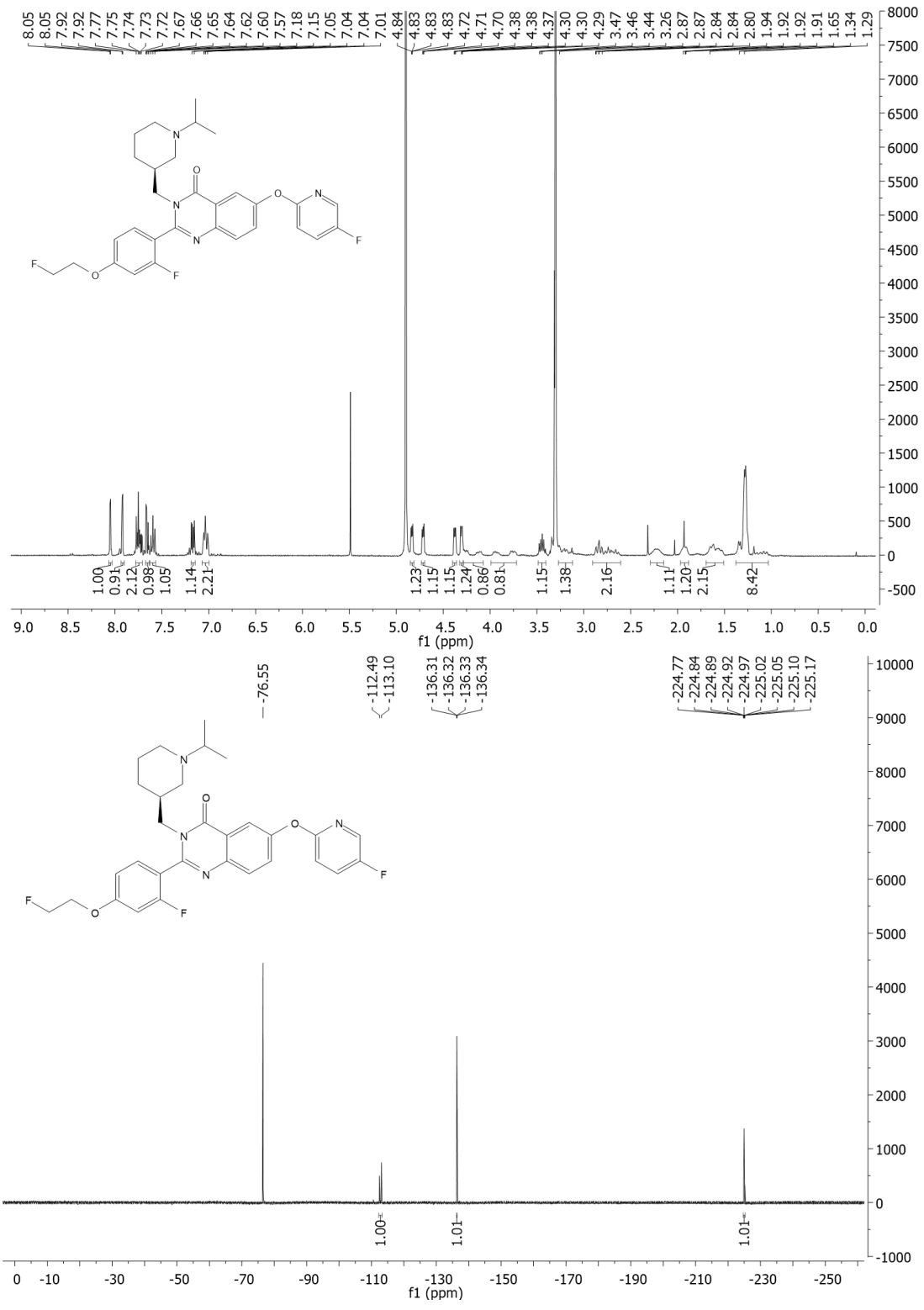
8.05 8.05 7.92 7.92 7.77 7.75 7.74 7.73 7.72 7.67 7.66 7.65 7.64 7.62 7.60 7.57 7.18 7.15 7.05 7.04 7.04 7.01 4.84 4.83 4.83 4.83 4.72 4.71 4.70 4.38 4.38 4.37 4.30 4.30 4.29 3.47 3.46 3.44 3.26 2.87 2.87 2.84 2.84 2.80 1.94 1.92 1.92 1.91 1.65 1.34 1.29
1.00 0.91 2.12 0.98 1.05 1.14 2.21 1.23 1.15 1.15 1.24 0.86 0.81 1.15 1.38 2.16 1.11 1.20 2.15 8.42
f1 (ppm)
-76.55
-112.49 -113.10
-136.31 -136.32 -136.33 -136.34
-224.77 -224.84 -224.89 -224.92 -224.97 -225.02 -225.05 -225.10 -225.17
1.00 1.01 1.01
f1 (ppm)

7b

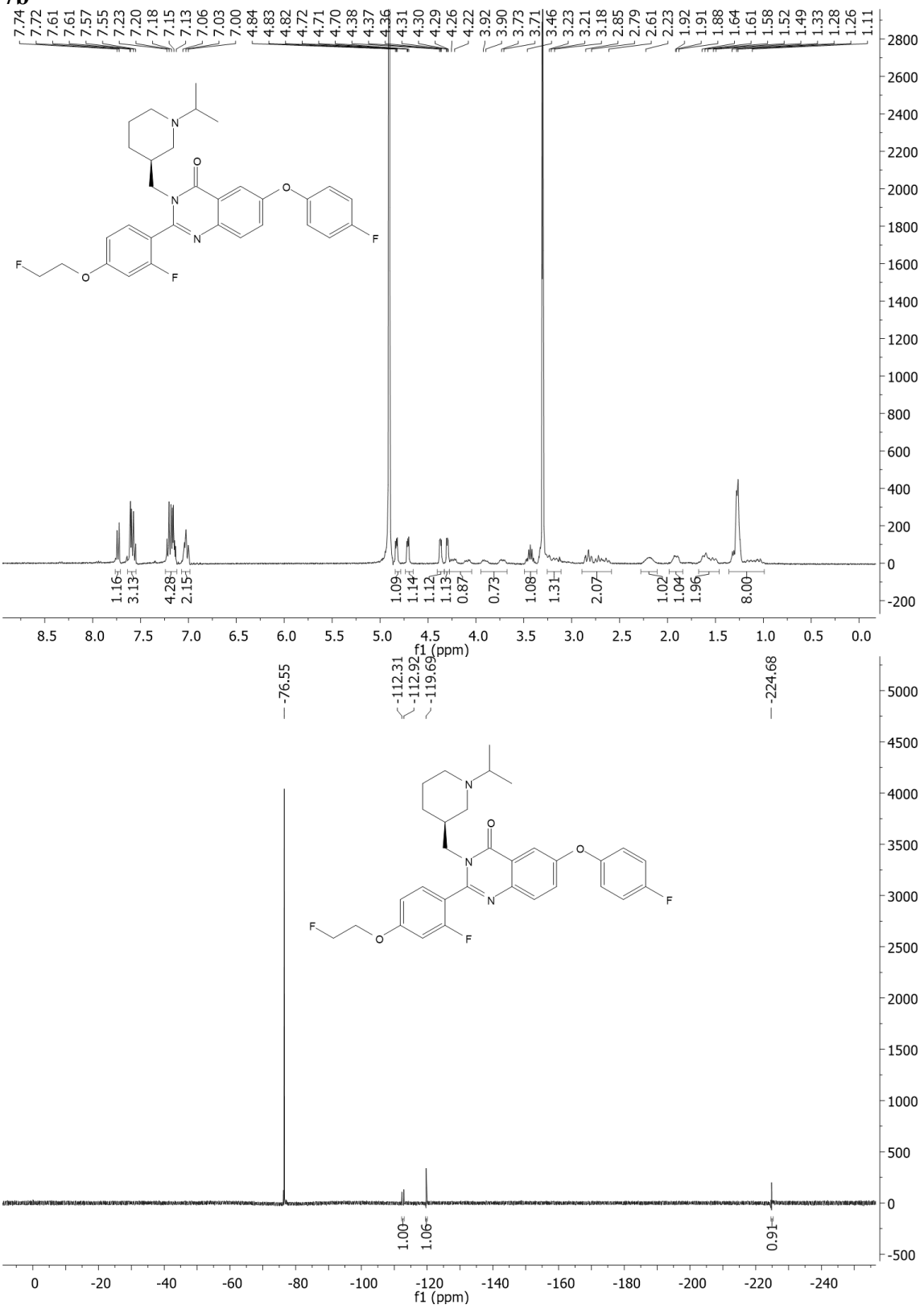
7.74 7.72 7.61 7.61 7.57 7.55 7.23 7.20 7.18 7.15 7.13 7.06 7.03 7.00 4.84 4.83 4.82 4.72 4.71 4.70 4.38 4.37 4.36 4.31 4.30 4.29 4.26 4.22 3.92 3.90 3.73 3.71 3.46 3.23 3.21 3.18 2.85 2.79 2.61 2.23 1.92 1.91 1.88 1.64 1.61 1.58 1.52 1.49 1.33 1.28 1.26 1.11
1.16 3.13 4.28 2.15 1.09 1.14 1.12 1.13 0.87 0.73 1.08 1.31 2.07 1.02 1.04 1.96 8.00
f1 (ppm)
-76.55 -112.31 -112.92 -119.69 -224.68
1.00 1.06 0.91
f1 (ppm)

Appendix C: Binding curves

ID	Compds.	Competitive binding curves
4a	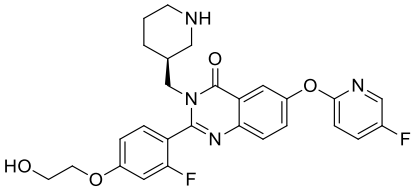	
4b	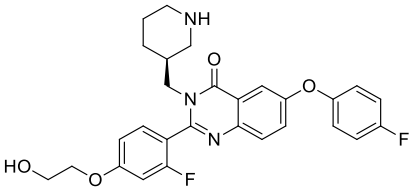	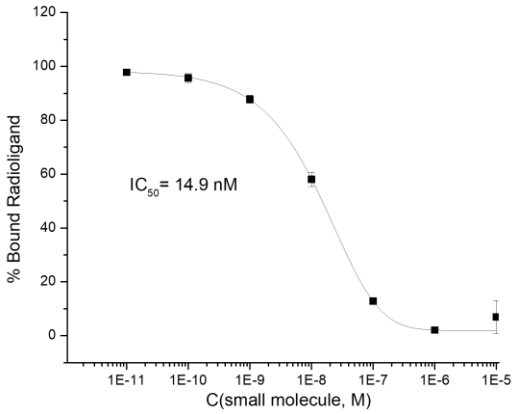
5a	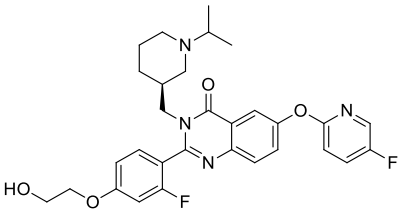	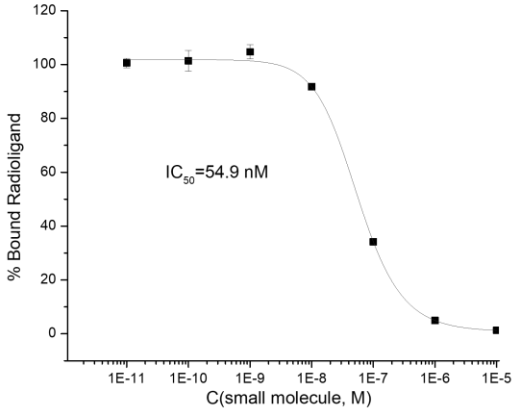
5b	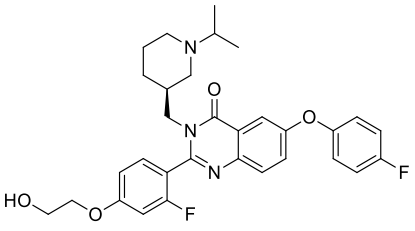	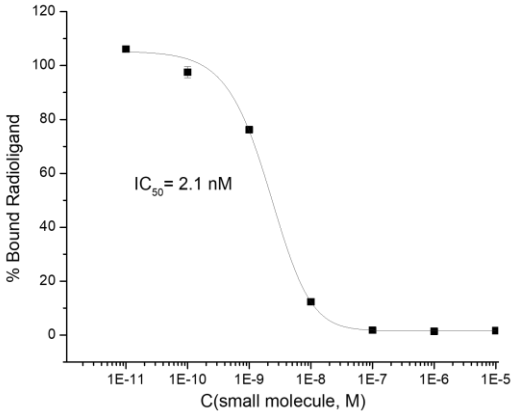

7a

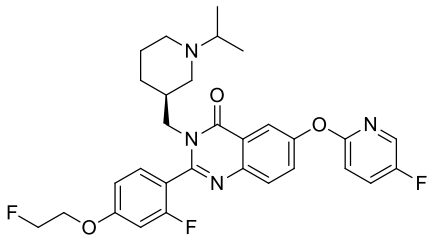

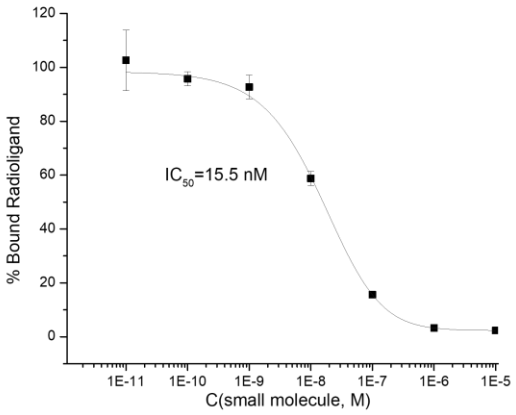

7b

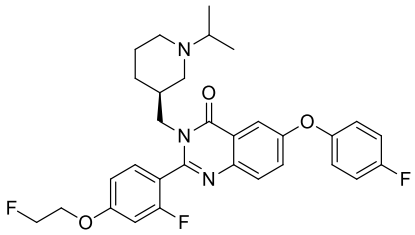

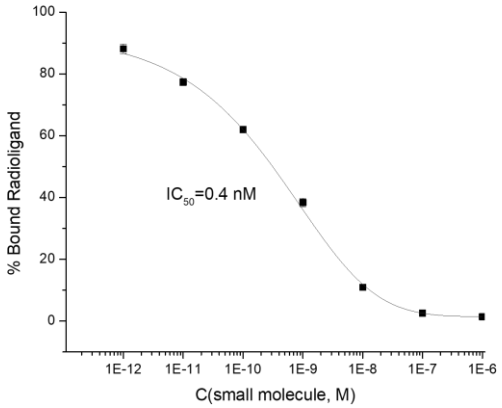

Ghrelin 1-28